Accepted Manuscript

Insight into factors controlling formation rates of pedogenic carbonates: A combined geochemical and isotopic approach in dryland soils of the US Southwest

CHEMICAL GEOLOGY

NOTIFIED TO THE STATE OF T

Syprose Nyachoti, Lixin Jin, Craig E. Tweedie, Lin Ma

PII: S0009-2541(17)30568-5

DOI: doi:10.1016/j.chemgeo.2017.10.014

Reference: CHEMGE 18503

To appear in: Chemical Geology

Received date: 17 March 2017
Revised date: 6 July 2017
Accepted date: 9 October 2017

Please cite this article as: Syprose Nyachoti, Lixin Jin, Craig E. Tweedie, Lin Ma, Insight into factors controlling formation rates of pedogenic carbonates: A combined geochemical and isotopic approach in dryland soils of the US Southwest. The address for the corresponding author was captured as affiliation for all authors. Please check if appropriate. Chemge(2017), doi:10.1016/j.chemgeo.2017.10.014

This is a PDF file of an unedited manuscript that has been accepted for publication. As a service to our customers we are providing this early version of the manuscript. The manuscript will undergo copyediting, typesetting, and review of the resulting proof before it is published in its final form. Please note that during the production process errors may be discovered which could affect the content, and all legal disclaimers that apply to the journal pertain.

Insight into factors controlling formation rates of pedogenic carbonates: a combined geochemical and isotopic approach in dryland soils of the US Southwest

Syprose Nyachoti¹, Lixin Jin¹*, Craig E. Tweedie², and Lin Ma¹

¹Department of Geological Sciences, University of Texas at El Paso, El Paso, TX 79968

²Department of Biological Sciences, University of Texas at El Paso, El Paso, TX 79968

* Corresponding author: ljin2@utep.edu, 500 W. University Ave., El Paso, TX 79968

Abstract

Natural accumulation of pedogenic carbonates has been well documented but few studies have focused on carbonate formation in agricultural drylands. This study aims to determine accumulation rates of pedogenic carbonates in intensively irrigated soils, and to define key linkages between flood irrigation, salt loading and soil-atmospheric CO₂ exchange in cultivated drylands of the southwestern United States. We used a combination of elemental chemistry (CaO, soil organic and inorganic carbon contents), mineralogy, and U-series (²³⁸U-²³⁴U-²³⁰Th) disequilibrium dating technique to investigate calcium sources, ages and formation rates of pedogenic carbonates. Study sites include an irrigated alfalfa field near El Paso in western Texas and a non-irrigated natural dryland site on the USDA Jornada Experimental Range of southern New Mexico. Our results showed that large amounts of dissolved calcium and inorganic carbon along with other soluble elements were loaded onto agricultural fields through irrigation waters in El Paso, TX while dust and rainfall were important for salt loading in natural soils of the Jornada. U-series activity ratios, (234U/238U) and (230Th/238U), in bulk soils suggested eolian deposits added U and modified U isotopes in shallow soils at both the irrigated and natural sites. Mobility of ²³⁴U within the soil profile is related to leaching of U (and by inference other soluble ions) and carbonate accumulation at depth. The U-series dating technique in pedogenic carbonates revealed the presence of much younger carbonates at the irrigated site compared to the natural site. Pedogenic carbonate formation rates in the irrigated soils were also much higher than those in the non-irrigated soils, likely a result of influxes from dissolved Ca and inorganic carbon in water used for irrigation. This study demonstrates the potential for agricultural expansion and land use change in drylands to increase rate of pedogenic carbonate accumulation. Such changes may have important implications to global carbon cycling since drylands are forecast to become the most expansive terrestrial biome by mid-century and dryland agriculture is expanding quickly.

Key words: dryland irrigation, salt loading, pedogenic carbonates, U-isotopes

1. Introduction

Pedogenic carbonates commonly form as secondary phases in dryland soils (Gile et al., 1981; Eswaran et al., 2000). This soil inorganic carbon pool is estimated to contain between 700 and 940 Pg C (1Pg = 10¹⁵g), a pool similar in size to atmospheric carbon (CO₂) and about two-thirds of the global soil organic carbon pool (Schlesinger et al., 1982; Eswaran et al., 2000; Monger and Martinez-Rios, 2001; Serna-Perez, 2006). Pedogenic carbonates develop when dissolved bicarbonate (HCO₃-) react with dissolved calcium (Ca²⁺) to form calcite (CaCO₃), carbon dioxide (CO₂) and water (H₂O):

$$2HCO_3^- + Ca^{2+} \rightarrow CaCO_3(s) + CO_2(g) + H_2O$$
 Rxn (1)

The precipitation of such secondary calcite is driven entirely by the availability of Ca²⁺ and HCO₃⁻ in soil water, and is thus controlled by local topography, rainfall, soil texture, and soil mineralogy (Lahann, 1978; Chadwick et al., 1989; Royer, 1999; Chiquet et al., 1999; Egli and Fitze, 2001; Hirmas et al., 2010; Laudicina et al., 2013). Improved understanding of the formation kinetics of pedogenic carbonates has important implications for erudition of the global C cycle, soil ages, formation of geomorphic surfaces, and reconstruction of paleo-environmental conditions (Cerling, 1984; Luo and Ku, 1991; Lal and Kimble, 2000; Serna-Perez et al., 2006).

Pedogenic carbonates take many forms in soils, ranging from coatings, nodules, to continuous hardpan calcrete (Machette, 1985; Violette et al., 2010) and have been grouped into different morphological stages of development (Gile et al., 1961; Machette, 1985; Monger et al., 1991; Birkeland et al., 1991). Dryland soils in the US Southwest contain abundant carbonates in various stages of development (Gile et al., 1981; Machette, 1985; Naiman et al., 2000). Samples of stage I to IV carbonates collected in the Jornada basin have provided key information on paleo-climate, paleo-vegetation, eolian processes, and geomorphic surface ages in southwestern New Mexico and western Texas (Gile et al., 1966; Gile and Grossman, 1979; Gile et al., 1981; Machette, 1985; Capo and Chadwick, 1999; Chiquet et al., 1999; Monger and Gallegos, 2000; Naiman et al., 2000; Deutz et al., 2002).

Climate- and human-induced changes have greatly impacted dryland landscapes. Sometimes, this has led to the degradation of surface hydrological conditions and soil properties and losses of ecosystem functions and services (Pimentel et al., 1995; Kummerer et al., 2010; D'Odorico et al., 2012). For example, soil salinization is a common form of land degradation, especially following irrigation (e.g., Schoups et al., 2005), which is essential for agricultural viability in dryland agricultural fields. Irrigated farming of the Rio Grande valley with relatively saline water from the Rio Grande and local groundwater (e.g., with total dissolved solids, or TDS, at ~1000 mg/kg) has prevailed for the past 100 years (Ellis et al., 1993; Moore et al., 2008; Miyamoto, 2012). In this region, high evapotranspiration rates and intensive irrigation using water with high TDS have combined to cause excessive salt accumulation, including calcite and most soluble evaporite minerals such as halite and gypsum (Cox, 2012; Cox et al., 2017). At a global scale, 4% of dryland surfaces (~ 2 million km²) are currently managed as irrigated agriculture, and almost 20% of irrigated drylands (0.4 million km²) have become salt affected, impacting crop growth and soil fertility (Dregne et al., 1991; Ghassemi et al., 1995).

Dryland agriculture probably alters rates of soil pedogenic carbonate accumulation and carbon sequestration (Saurez, 2000; Schlesinger, 2000; Sanderman, 2012). The presence of high concentrations of calcium and bicarbonate ions in irrigation water could lead to calcite saturation and precipitation in agricultural soils. This could affect soil quality through a reduction in soil porosity and impairment of water infiltration and plant root penetration (Entry et al., 2004; Ontl and Schulte, 2012; Sanderman, 2012). However, few studies have examined the kinetics of calcite deposition in these managed systems (Saurez, 2000; Schlesinger, 2000; Sanderman, 2012).

Here, we compare carbonate formation rates in soils of a natural dryland site at the USDA Jornada Experimental Range, in southern New Mexico and a nearby irrigated agricultural site (alfalfa) close to El Paso, Texas (Fig. 1). The non-cultivated site at Jornada contains voluminous pedogenic carbonates that have formed naturally in the absence of irrigation. Thus, the Jornada site provides an ideal baseline for assessing the likely rates of carbonate accumulation in irrigated agricultural soils. This study uses elemental chemistry, mineralogy, uranium-series isotopes, and published calcium carbonate loads in soils of the US

Southwest to: (1) identify sources of calcium and carbon and quantify their influxes to soils, (2) constrain ages of pedogenic carbonates, and (3) estimate and compare long-term averaged carbonate formation rates in natural and managed soils of the US Southwest.

2. Background on U-series isotope dating of pedogenic carbonates

Pedogenic carbonates can be dated using a U-series isotope disequilibrium technique (Ku et al., 1979; Ludwig and Paces, 2002; Sharp et al., 2003). The U-series dating technique relies on the relationship between radioactive decay of the parent and ingrowth of the daughter isotopes in the U-series chain (e.g. 238 U, 234 U, and 230 Th). For example, 238 U ($t_{1/2}$ = ~4.5 Gyrs) decays to a relatively short-lived 234 U ($t_{1/2}$ = ~246 kyrs) that subsequently decays to 230 Th ($t_{1/2}$ = 76 kyrs) (Dickin, 1995; Cheng et al., 2000). The upper limit of the carbonate ages that can be dated by the U-series technique is approximately 0.6 Ma (Cheng et al., 2016).

The activity ratios of the U-series isotopes, e.g. (234U/238U) and (230Th/238U) (herein indicated by parenthesis) in a closed system for more than 1.25 Ma will be equal to unity, also known as secular equilibrium. During water-rock interaction, U-series isotopes are fractionated (Vigier et al., 2001; Chabaux et al., 2003; Chabaux et al., 2008; Dosseto et al., 2008). For example, due to the high solubility of U in oxidizing environments, direct alpha recoils, and preferential leaching of 234U through alpha recoil effects, weathering fluids such as soil water usually have high U concentrations and (234U/238U) ratios. On the other hand, soil waters in similar environments are characterized with very low Th concentrations and (230Th/238U) ratios due to the low solubility of Th (Langmuir and Herman, 1980). Precipitation of secondary minerals such as pedogenic carbonates from soil water results in deposits with (234U/238U) greater than one but with low concentrations of 230Th. Thus the measurable 230Th in the carbonates is assumed to be from the decay of 234U over time (Ivanovich and Harmon, 1992; Andersen et al., 2008). However, pedogenic carbonates usually include U and Th from detrital silicate fractions; such contamination requires additional

corrections for U-series disequilibrium dating (Bischoff and Fitzpatrick, 1991; Edwards et al., 2003; Neymark, 2011).

The isochron technique is commonly employed for correction of detrital ²³⁰Th in pedogenic carbonates (Ku et al., 1979; Edwards et al., 2003; Sharp et al., 2003); Paces et al., 2012). This method requires the use of cogenetic samples that may be obtained by applying leachate/residue, leachate/leachate, or total sample dissolution methods on bulk pedogenic carbonates (Bischoff and Fitzpatrick, 1991; Edwards et al., 2003; Neymark, 2011). It is important to note that this correction technique takes the following assumptions into consideration: 1) the pure carbonates precipitating from soil water contain no Th due to its low solubility; 2) there are only two isotopically homogeneous end members in pedogenic carbonates: detrital materials and authigenic carbonates; and 3) the system remains closed to U and Th after formation of carbonates (Bischoff and Fitzpatrick, 1991; Luo and Ku, 1991). In general, (²³⁰Th/²³²Th), (²³⁸U/²³²Th), and (²³⁴U/²³⁸U) ratios in cogenetic samples are used to construct 2D isochrons (Osmond et al., 1970; Rosholt, 1976) and to infer (²³⁴U/²³⁸U) and (²³⁰Th/²³⁸U) ratios of the pure authigenic carbonate for age calculations (e.g. Ludwig, 2003).

3. Methods

3.1. Site description

The study sites include an irrigated alfalfa field near El Paso, Texas (31.6729886°N, 106.2667956°W) and a natural non-irrigated shrubland in the Jornada basin near Las Cruces, New Mexico (32.565500°N, 106.659800°W) (Fig. 1; Appendix Figs. 1, 2, and 3). Both sites are located within the Rio Grande valley system, which comprises a number of north-south trending inter-montane basins that are part of the Cenozoic-age Rio Grande tectonic system (Hawley and Kennedy, 2004).

Agricultural soils in western Texas are generally developed on alluvium deposits of the Rio Grande valley and are classified as Entisols and Aridisols (Miyamoto and Chacon 2006). These floodplains belong to the Holocene Fillmore geomorphic surface (100 yrs to 7000 yrs B.P) in the Hueco basin, where the

irrigated Alfalfa site is located (Gile et al., 1981). Field survey by soil pits and augered cores revealed that the shallow soils (<1 m depth) of the irrigated Alfalfa site consisted of a fine silty clay loam or clayey loam (Appendix Figure 1), overlying a silty-loamy layer at ~1 to 4 m depth (USDA-TAES, 1971; Miyamoto, 2012). The calcite content in these river alluvial sediments is shown to be variable, range from non-existent to cements around the sands and pebbles (Hawley and Lozinsky, 1992), and is assumed to be negligible in the parent sediments in the Alfalfa site.

The climate of the region is semi-arid with a low mean annual precipitation of ~25 cm and mean annual temperature of 18°C (USDA-TAES, 1971). The soils of the cultivated alfalfa field used in this study are irrigated regularly between April and October. During irrigation season, the field is generally flood irrigated every two weeks to an extent that permits standing water for about one week. Irrigation water is sourced from Rio Grande River, an important freshwater resource in the US Southwest (Ellis et al., 1993). The salinity of the Rio Grande increases from headwaters in Colorado (Phillips et al., 2003; Hutchison, 2006; Hogan et al., 2007; Szynkiewicz et al., 2011) to southern New Mexico and western Texas. At El Paso, the salinity of the Rio Grande is about 800 to 2000 mg/l, and varies seasonally and with river discharge (Szynkiewicz et al., 2015). River water is saturated with respect to calcite but under-saturated with respect to evaporite minerals such as gypsum and halite (Szynkiewicz et al., 2011).

The non-irrigated natural site used in this study (Jornada) was situated in the Jornada basin on the US Department of Agriculture's Jornada Experimental Range (JER) in a zone free of any agricultural activities (Serna-Perez et al., 2006). The Jornada site is located on the piedmont slopes of mountain ranges within the Rio Grande Rift (Keller et al., 1990; Serna-Perez et al., 2006). The basin is filled with ~ 2000 m thick marine and non-marine sediments (mostly piedmont alluvium, lacustrine materials), which are overlaid by ~150 m of late Tertiary and Quaternary ancestral Rio Grande and eolian deposits (Gile et al., 1981; Mack et al., 1997; Monger, 2006). These young sediments, which form the parent material of soils in the Jornada basin (Gile et al., 1966; Seager et al., 1987; Mack and James, 1992; Monger and Gallegos, 2000), include a mixture of clay, silt, sand, and pebbles and contain <1% calcite. The soils on the Jornada I geomorphic surface contain well-developed petrocalcic horizons ("Caliche") with stage IV and V

carbonates (Appendix Figs. 2 and 3), which are either preserved in deep soil layers or exhumed by wind or water erosion (Gile et al., 1981; Machette, 1985). The age of the Jornada I geomorphic surface is approximately 500 to 700 ka (Monger et al., 2009). The Jornada basin receives approximately 21-25 cm of precipitation each year, mostly during the summer monsoon. The annual potential evapo-transpiration at the Jornada basin is approximately 220 cm and mean annual temperature is ~16 °C (Gile et al., 1981). Vegetation at the Jornada basin has changed through time (Gibbens et al., 2005), and is currently dominated by the C3 shrubs mesquite (*Prosopis glandulosa*) and creosote bush (*Larrea tridentata*) (Gibbens et al., 2005; Serna-Perez et al., 2006; Bergametti and Gillette, 2010).

3.2. Soil and caliche sample collection

Soil samples were collected from a pit at the Alfalfa field as previously described by Cox (2012) and Cox et al. (2017). Briefly, soil samples were collected at 10 cm intervals from the wall of the pit until 60 cm depth where a change from silt/clay to sandy soil texture was observed (field and sample photos in Appendix Fig. 1). In general, irrigated Alfalfa soil samples consisted of sand to clay sized particles with large soil aggregates (~cm size), roots, and very fine carbonate nodules, films and filaments (<1 mm size). At the Jornada site, two ~50-cm deep pits were dug at approximately 5 m apart (JPT1 and JPT2; field and sample photos in Appendix Figs 2 and 3). JPT2 was located beneath a shrub while JPT1 was located between two mesquite shrubs. Soil samples were collected at 5 cm interval from land surface to the upper boundary of the caliche layer at each pit (40 and 48 cm at JPT1 and JPT2, respectively). The soil samples from the JPT soil pits consist of small gravels (<1cm), sands, silts, and clay-size particles. The gravels are generally coated with a thin layer of carbonates while fine carbonate nodules are abundant in the soil matrix.

Two caliche samples were collected from the bottom of the two soil pits (one from 40 cm depth at JPT1 and the other from 48 cm depth at JPT2; pictures given in Appendix Figure 2 and 3). The caliche layers are dominated by large gravels (\sim 5 to 10 cm) with \sim 1 cm-thick carbonate coatings. The carbonate layers do not show any lamination features. For each sample, five randomly selected points on the caliche

surface were scrapped off to obtain enough materials for total sample digestion (samples were assumed to be coeval). Pictures of the field sites and location of sub-sampled caliche are included in Appendix Figures 2 and 3. Hereon, 'caliche' refers to these subsamples.

3.3. Soil major element chemistry and mineralogy

For major element analysis, the soils were air dried, ground to pass through a 100-mesh sieve (<150μm), and digested using a Li-metaborate fusion technique (Feldman, 1983). Specifically, 0.1 g ground soil powder and 1g lithium metaborate were weighed and mixed using a mixer mill (Spex sample prep 5100) before digestion in a muffle furnace at 900°C for 15 minutes. The molten bead was then completely dissolved in 5% nitric acid, and the solution was diluted and analyzed for major elements using a Perkin-Elmer Optima 5400 inductively coupled plasma optical emission spectrometer (ICP-OES) at the University of Texas at El Paso (UTEP). Twenty rock standards from NIST and USGS were digested using the same procedure and used as calibration standards for major elements along with a procedure blank. A USGS reference rock material (W-2) was digested with each batch of soil samples as a quality check. The difference between measured and certified values in all major element concentrations on W-2 were less than 10%.

Total soil carbon (SC) contents were measured from the powdered soils using a LECO SC632 carbon and sulfur determinator at UTEP. In addition, soil organic carbon (SOC) content was determined on the SC632 after soil inorganic carbon (SIC, or carbonate minerals) was removed by leaching with 10 ml of 10% HCl. The SIC was then calculated as the difference between SC and SOC. One ore tailing standard, one synthetic carbon standard, and a pure calcium carbonate sample were used as calibration standards. The uncertainties estimated from duplicates were less than 10%.

The dominant minerals in soils were identified by a MiniFlex II X-ray diffractometer at UTEP. The powdered samples were scanned from 5° to 65° 20 at 30 kV voltage and 15 mA current with Cu-K_{\alpha} radiation and a scintillation counter detector. Diffraction patterns were collected at a sampling width of 0.020° 20 and analyzed by peak matching with reference intensity ratios.

3.4. U-series isotope analysis of bulk soils and caliche pedogenic carbonates

For soils with fine carbonate nodules in the sample matrix, a combined leachate-residue procedure was applied to obtain sub-samples with various mixing ratios of detrital and pure carbonate end-members for U-series isotope analysis. Specifically, for each soil sample, three 100 mg aliquots were weighed and prepared as follows. The first aliquot was analyzed as a bulk soil after total digestion with HNO₃+HF+HClO₄ acids. For the second aliquot, approximately 10 ml of 0.1M HCl were added and the mixture was allowed to settle for 30 min and then centrifuged. The acid leachate (HCl-L) and residue (HCl-L) R) were then separated into beakers. Lastly, 10 ml of de-ionized water (18.2M Ω) were added to the third aliquot and the mixture was allowed to settle for 10 min and centrifuged. The water leachate (H₂O-L) and residues (H₂O-R) were put into separate beakers. The caliche, bulk soil, leachate and residue samples were then analyzed for isotopic compositions and concentrations of U and Th following procedures detailed in Granet et al. (2007) and Pelt et al. (2008). Specifically, after ²³³U and ²²⁹Th spikes were added to the samples, all samples were evaporated to near dryness and completely digested with HNO3+HF+HClO4 acids and H₃BO₃+HCl for ~ 48 hrs prior to column separation in a class-100 clean room. U and Th in the samples were separated and purified from the matrix using AG 1-X8 anion exchange resin (200-400 mesh). Isotopic ratios (234U/238U, 233U/238U, 235U/238U, 230Th/232Th, and 229Th/232Th) were measured using a standard-sample bracketing method on a Nu Plasma HR MC-ICP-MS at UTEP. The NBL U145B solution was used as the U bracketing standard to correct for mass fractionation and to calculate ion counter gains for U isotope ratio measurements (234U/238U, 235U/238U, and 233U/238U). A 229-230-232Th in-house standard that was calibrated against an IRMM 035 solution was used as the Th bracketing solution for Th isotope ratio measurements (230Th/232Th and 229Th/232Th). U and Th concentrations were calculated using measured ²³³U/²³⁸U and ²²⁹Th /²³²Th isotope ratios by the isotope dilution method, respectively. Activity ratios (234U/238U) and (230Th/232Th) were calculated from measured 234U/238U and 230Th/232Th isotope ratios. Accuracy of measurements was assessed regularly by analyzing the USGS W2 rock reference material. The measured average U and Th concentrations of W2 over the term of analysis were: $U = 0.503 \pm 0.014$ ppm

 $(n = 8, 2\sigma)$ and Th = 2.148 ± 0.001 ppm $(n = 7, 2\sigma)$; all within the reported reference values (Sims et al., 2008). Measured U-series activity ratios of the W-2 reference material were at secular equilibrium as expected (see Results). Uncertainties in $(^{234}\text{U}/^{238}\text{U})$ and $(^{230}\text{Th}/^{232}\text{Th})$ activity ratios were 5‰ (1σ) and 1% (1σ) , respectively. U and Th procedure blanks were ~4 pg and ~100 pg and considered negligible.

3.5. ¹⁴C analysis of pedogenic carbonates

Two soil samples, Alfalfa (40-43cm) from irrigated site and JPT2 (27-30cm) from the natural site, were analyzed at the Center for Applied Isotope Studies at the University of Georgia for ¹⁴C radiocarbon ages. These samples were chosen because their U-series ages lie within the limits of the radiocarbon dating technique (<30 ka). For the analysis, carbon dioxide was released from pedogenic carbonates in the soil samples using phosphoric acid in a vacuum. The carbon dioxide was purified and converted to graphite following procedures detailed in Vogel et al. (1984). The ¹⁴C/¹³C ratios of graphite were measured using the CAIS 0.5 MeV accelerator mass spectrometer and compared to that measured from the Oxalic Acid I (NBS SRM 4990). Apparent radiocarbon ages were reported in years before 1950 (years BP) after correcting for isotopic fractionation. The statistical and experimental errors are reported to one standard deviation.

4. Results

4.1. Soil mineralogy and major element chemistry

The dominant minerals observed in all soil samples were quartz, calcite, feldspars and clays. Calcite is more abundant in the natural Jornada soils than the irrigated Alfalfa soils, especially at depth (Table 1). Calcite/quartz abundance ratios, expressed as intensity ratios of peak 29.42° 20 (calcite) and peak 26.65° 20 (quartz) on a XRD spectrum, varied little with depth at three soil profiles between two sites, but increased sharply in samples from JPT1 and JPT2 when soils transition to the caliche layer (Fig. 2a). The soil inorganic carbon (SIC) contents in all soil and caliche samples range from 0.50 to 8.73 wt%, and show

similar depth trends as calcite/quartz ratios through XRD (Fig. 2b; Table 1). The content of SIC increased from 3.88 wt% in 25-30 cm soil to 8.73 wt% in calcihe at the JPT1 site; similarly, the SIC content increased from 1.86 wt% in 37-40 cm soil to 5.39 wt% in calcihe at the JPT2 site (Table 1). Based on $CaCO_3$ stoichiometry, caliche at JPT1 and JPT2 were $\sim 73 \text{ wt\%}$ and $\sim 45 \text{ wt\%}$ calcite respectively.

The soil organic carbon (SOC) content at the Alfalfa and Jornada sites (0.07 to 0.82 wt%) was generally greatest near the soil surface (Fig. 2d). The JPT2 soils had higher SOC content than the JPT1 soils, possibly because JPT2 was located underneath a shrub while JPT1 was situated between two shrubs. The total soil carbon (SC) content at the Jornada site (3.0-9.1 wt% at JPT1 and 1.5- 6.6 wt% at JPT2) was higher than those documented at the Alfalfa site (0.6-1.7 wt%) (Table 1; Fig. 2c). The SC pool at the Alfalfa site was comprised of approximately equal amounts of SOC and SIC, while the SC pool at the Jornada site is dominated by SIC (Figs. 2b, c, d).

At the Jornada site, calcium oxide (CaO) concentrations ranged from 12.7 to 45.6 wt% at JPT1 and from 9.9 to 46.2 wt% at JPT2 (Table 1; Fig. 3). The highest CaO concentrations were observed in the caliche samples taken at the bottom of the JPT1 and JPT2 pits. The CaO concentrations at the Alfalfa soils were much lower, ranging from 2.9 to 5.4 wt%. The CaO contents in soils can potentially come from carbonate and silicate minerals. The measured SIC and CaO contents in these soils were used to estimate the weight percentages of CaO contribution from calcite (based on stoichiometry of CaCO₃ and SIC content) vs. CaO contribution from silicates such as feldspars and clays (difference from total CaO and those from calcite). On average, approximately 80% of the CaO in alfalfa soils is present as calcite. The percentages increase to 89 to 100% at JPT1. In contrast, only about 50-65% of CaO is present as calcite at the JPT2 site, with a higher contribution from silicate minerals (Table 1; Figure 3). Such a difference could be due to the presence of different amounts of large gravels and rock fragments, that are fluvial sediments of Ca-bearing silicate rocks at these sites (Appendix Figures 2 and 3).

4.2. U and Th concentrations and activity ratios in bulk soils

The U concentrations in bulk soils ranged from 1.1 to 2.0 ppm (mg/kg) at JPT1 and 1.3 to 2.0 ppm at JPT2 (Table 1). The Th concentrations in bulk soils ranged from 2.3 to 8.7 ppm at JPT1, and 1.6 to 8.7 ppm at JPT2 (Table 1). The lowest U and Th concentrations were observed in caliche samples at the bottom of the soil pits at the Jornada sites and generally increased in bulk soils toward the soil surface (Table 1). However, U/Th ratios decreased towards the soil surface in these two profiles (Figs. 4a,b). The U and Th concentrations in bulk soils of the Alfalfa site were within a similar range of those at Jornada but showed little variation with depth.

The (²³⁴U/²³⁸U) ratios in bulk soils showed distinctively different depth profiles between the Jornada and Alfalfa sites. At the Jornada sites, (²³⁴U/²³⁸U) ratios increased from 0.95 to 1.00 with increasing depth, and became much higher (1.18-1.30) at the caliche layer (Fig. 4c). At the Alfalfa site, the (²³⁴U/²³⁸U) ratios decreased from 1.02 to 0.97 with increasing depth (Fig. 4d).

The $(^{230}\text{Th}/^{238}\text{U})$ ratios were > 1 in all bulk soils at the Jornada site, except for the two caliche samples with $(^{230}\text{Th}/^{238}\text{U})$ ratios < 1 (0.75 to 0.92) (Fig. 4e). Similarly, $(^{230}\text{Th}/^{238}\text{U})$ ratios were > 1 in bulk soils at the Alfalfa site, except for the sample at 53cm depth with a $(^{230}\text{Th}/^{238}\text{U})$ ratio <1 (0.75) (Fig. 4f). Bulk soil $(^{230}\text{Th}/^{238}\text{U})$ ratios in all Jornada and Alfalfa profiles increased toward the land surface (Figs. 4e,f).

4.3. U and Th activity ratios in pedogenic carbonates

The HCl leachates (HCl-L) showed distinctively lower (²³²Th/²³⁸U) ratios and higher (²³⁴U/²³⁸U) ratios than their corresponding HCl residues (HCl-R) of the bulk soils at both the Alfalfa and Jornada sites (Table 2 and Appendix Figure 4). This is consistent with the fact that the weak acids (i.e., 0.1 M HCl) hydrolyzed carbonates whereas the acid-leached residues contained mainly detrital silicate materials. The water-suspended portions (H₂O-L) of the bulk soils generally showed higher (²³²Th/²³⁸U) ratios than the residual portions (H₂O-R), probably because water-suspended portions were relatively enriched in fine detrital silicate particles such as clays in comparison to the residual portions (H₂O-R). Based on the U-series activities ratios, both acid leachate-residue and water suspension procedures created sub-samples with different proportions of carbonate versus detrital end-members (Table 2 and Appendix Figure 4).

The bulk caliche samples had (²³⁴U/²³⁸U) ratios >1 and (²³⁰Th/²³⁸U) ratios <1 (Table 1), consistent with the dominance of pedogenic carbonates in the bulk samples. The relatively high (²³²Th/²³⁸U) ratios of these caliche samples were due to the presence of a significant detrital component, consistent with the brown to dark brown spots observed in the white carbonate matrix. For each caliche sample, one gravel sample was used to obtain sub-samples with different proportions of carbonate versus detrital end-members. The carbonate coatings on these gravels did not show any apparent laminated layers or features that could be used to infer growth directions or history. Hence, five random spots were selected on the outermost surface layer of the carbonate coating for analysis (Appendix Figures 2 and 3). These scrapped carbonate powders all showed relatively large variations in (²³⁴U/²³⁸U), (²³⁰Th/²³⁸U), and (²³⁸U/²³²Th) ratios (Table 2), due to the presence of various amounts of detrital components in sub-samples.

4.4. Estimation of pedogenic carbonate ages with isochrons

The U-series isotope signatures of the ideal pure carbonate end-member in bulk soils or caliches and then their ages were derived from the typical isochron diagrams described in the section above (e.g. Rosholt type or Osmond type; Ludwig, 2003). The Osmond type isochron diagrams (230 Th/ 238 U vs. 232 Th/ 238 U and 234 U/ 238 U vs. 232 Th/ 238 U) for both the Alfalfa and Jornada sites showed strong linearity (R² = 0.52 to 0.99) for all soil and caliche samples (Table 2 and Appendix Figure 4), except for samples from Alfalfa 60-63cm, JPT1 10-15 cm, and JPT2 0-7 cm. Isoplot III was used to calculate carbonate ages and (234 U/ 238 U) $_0$ (U isotopic composition when carbonate formed initially) of pedogenic carbonates (Ludwig, 2003). The software calculates both age and its uncertainty using the measured and detrital corrected (234 U/ 238 U) and (230 Th/ 238 U) activity ratios, 234 U and 230 Th decay constants and the associated errors (Ludwig, 2003). In summary, pedogenic carbonate ages ranged from 2.2 ± 1.7 ka to 15 ± 17 ka for Alfalfa soils, 14.5 ± 6.8 ka to 117 ± 26 ka for Jornada JPT1, and 19.5 ± 7.5 ka to 100 ± 40 ka for Jornada JPT2 (Fig. 5; Table 1). In general, samples with poor linearity in the isochron diagrams (e.g. JPT2 0-7cm) also had large age uncertainties, suggesting that these samples were mixtures of more than one carbonate end-member and one detrital end-member. However, for the rest of the samples with good linearity in the

isochron diagrams, the uncertainty of age was also large, probably due to the nature of the study sites. First, it was impossible to physically separate pure carbonate minerals from the detrital matrix in bulk soil samples (Appendix Figures), and secondly, carbonates in bulk soils and caliche samples had different growth histories (e.g., at ~10 cm sampling depth interval). Thus, the ages reported from U-disequilibrium series are probably mass-weighted averages of carbonates that are a mixture of ages in any given sample, which resulted in large age uncertainties. Despite the large uncertainties, ages of carbonates in bulk soils at JPT1 and JPT2 were generally greater than those from the Alfalfa profile and the two caliche samples from the Jornada had the oldest pedogenic carbonates among all the samples analyzed in this study (Fig. 5).

4.5. Comparison of the U- series and radiocarbon carbonate ages

Apparent radiocarbon ages were reported for the two bulk soil samples in Table 1: the carbonates in the Alfalfa 40-43 cm sample had an apparent radiocarbon age of 6.54 ± 0.03 ka, older than the U-series age for this sample $(2.2 \pm 1.7 \text{ ka})$. Carbonates in the JPT2 27-30cm sample yielded a radiocarbon age of 8.36 ± 0.03 ka, younger than their U-series age documented for the same sample (19.5 \pm 7.5 ka). Below we discuss possible reasons why radiocarbon and U-series ages were different for these two bulk soil samples. Just like U-series isotopes, ¹⁴C is extremely useful for dating pedogenic carbonates (e.g., Amundson et al., 1994; Pustovoytov et al., 2007). However, it remains poorly understood how the addition of dead carbon from old soil organic matter or carbonate materials can potentially introduce much older ages (e.g., Wang et al., 1994; Amundson et al., 1989; Monger et al., 1998). If pedogenic carbonate dissolved and reprecipitated in soils, its ¹⁴C system would equilibrate with the ¹⁴C signature of 'young' soil CO₂, leading to higher ¹⁴C activity and thus younger radiocarbon ages (e.g., Kuzyakov et al., 2006). As discussed above, bulk soils are a mixture of pedogenic carbonates of different ages. The half-life of ¹⁴C is different from those of the U-series isotopes, and thus the non-linear mixing of different carbonates may lead to a substantial deviation from the radiocarbon age determined from the U-series. We have no additional evidence to support any of these mechanisms and the direct comparison of the apparent radiocarbon ages to the U-series ages is beyond the scope of this study. More detailed studies focused on calibrating ages

from multiple dating techniques in pedogenic carbonates are needed. Even with the discrepancies, both the apparent radiocarbon ages and the U-series ages showed that the JPT2 sample had older carbonates than the Alfalfa sample.

5. Discussion

5.1. Behavior of U-series isotopes in soil profiles

U-series isotope ratios in bulk soils reflect contributions from both pedogenic carbonates and detrital silicates. During water-rock interaction, alpha recoil effects and consequent damages in crystal lattices preferentially release ²³⁴U over ²³⁸U from bulk siliceous soils to soil waters, disturbing the secular equilibrium of (²³⁴U/²³⁸U) and (²³⁰Th/²³⁸U) activity ratios (e.g. Chabaux et al., 2003; Oster et al., 2012; Oster et al., 2017). Due to the high solubility of U in oxidizing environments and the preferential leaching of ²³⁴U, soil waters usually have high U concentrations and (²³⁴U/²³⁸U) ratios >1. Solubility of Th is low in similar environments, leading to (²³⁰Th/²³⁸U) ratios <1 in soil waters (Langmuir and Herman, 1980). Bulk silicate fractions of soils, as the residual phase after water-rock interaction, generally have (²³⁴U/²³⁸U) ratios < 1 and (²³⁰Th/²³⁸U) > 1. Precipitation of secondary minerals such as pedogenic carbonates carry similar isotopic signatures as those of soil waters (i.e., (²³⁴U/²³⁸U) > 1 and (²³⁰Th/²³⁸U) < 1). The secondary carbonate phases and the siliceous residues combine to control the mass balance of U-series isotopes in bulk soils.

The (²³⁴U/²³⁸U) ratios in Jornada bulk soils are all <1 and decrease toward the surface; (²³⁰Th/²³⁸U) values are >1 and increase toward the surface; elemental U/Th ratios also decrease toward the surface (Fig. 4). Such trends are consistent with the expected mobility of U-series isotopes in siliceous soils during chemical weathering and result in the preferential loss of ²³⁴U and ²³⁸U and accumulation of ²³⁰Th and ²³²Th in shallow soils. Thus, the U-series mass budget in these bulk soils is dominated by siliceous components with minor contributions from pedogenic carbonates. In contrast, the two caliche samples at depth (40 and 48 cm below land surface at JPT1 and JPT2, respectively), are dominated by carbonates and have

(²³⁴U/²³⁸U) values >1 and (²³⁰Th/²³⁸U) ratios <1. This isotopic signature agrees well with the likely scenario that U and Th dissolved in soil water during weathering and were re-precipitated during secondary mineral phases as pedogenic carbonate (Fig. 2).

Similar depth trends of (²³⁰Th/²³⁸U) and U/Th ratios are observed in the Alfalfa soils, suggesting U in Alfalfa soils reside mainly in silicate components, with minor contributions from secondary carbonates. However, the (²³⁴U/²³⁸U) ratios of the Alfalfa soils increase toward the surface, an opposite trend to the Jornada soils. Such a difference between natural and irrigated soils suggests that U is most likely added to soils from an external source such as irrigation water with higher (234U/238U) activity ratios. Indeed, the Alfalfa site is irrigated intensively with Rio Grande water that has high U concentrations (e.g., 3.3 to 5.6 ppb) and high (²³⁴U/²³⁸U) ratios (1.6 to 2.2) (Szynkiewicz et al., 2015; Nyachoti, 2016). Intensive water loss through evapotranspiration makes soil water oversaturated with respect to calcite, leading to precipitation of pedogenic carbonates in the agricultural fields (Cox, 2012; Cox et al., 2017). Dissolved U has a high affinity for bicarbonate ions (e.g. forming uranyl carbonates) and tends to precipitate along with carbonates (e.g. review by Chabaux et al., 2003). Irrigation-induced U can be incorporated into secondary calcite and become an important component in U mass balance, leading to higher (234U/238U) ratios in bulk soils. In addition to irrigation water. U from fertilizers in this region shows (234U/238U) ratios of ~1.0 (Szynkiewicz et al., 2015). This is higher than the bulk soil (234U/238U) ratios at depth at the Alfalfa site and could be another source of external U. The bulk Alfalfa soils at the 50-53 cm depth have a (230Th/238U) ratio <1, similar to the two caliche samples from the Jornada site. These observations suggest the formation of pedogenic carbonates is important for U mass balance at the Alfalfa site where U is leached from bedrock or parent materials through chemical weathering, U contributions are made from external sources (irrigation water and fertilizers), and the resulting pool of U is incorporated in bulk soils due to the formation of pedogenic carbonates.

5.2. Accumulation of pedogenic carbonates in natural and agricultural soils

5.2.1. Depth profiles of pedogenic carbonates

Quantification of soil carbonates as soil inorganic carbon and calcium contents are shown in Figures 2 and 3 for both the natural (Jornada) and the managed agricultural (Alfalfa) soils. Because of the lack of primary carbonates in parent sediments and bedrock at both sites (except for carbonates arriving in the form of dust), soil carbonates are predominantly of pedogenic origin. The Jornada soils (JPT1 and JPT2) have much higher carbonate contents than the Alfalfa soils (Figs. 2, 3). At the bottom of the Jornada soil pits, secondary calcite hardpan (or caliche) is especially well developed and were impenetrable by auger or shovel. The samples collected from the upper boundary of the thick caliche layer contain ~ 5.4 to 8.7 wt% of SIC, or the equivalent of 45 to 73 wt% of calcite (Fig. 2b). For shallow soils above the caliche layer, pedogenic carbonates, at 10 to 30 wt%, mainly occur as fine nodules in the soil matrix or as a thin coating on small gravels (Appendix Figure 2 and 3).

Carbonate concentrations are constant (about 10% wt% of calcite) in the upper 60-cm soil profile at the Alfalfa site, which is a much lower than that recorded in Jornada soils. The carbonates are present as fine particles or coating in the soil matrix at the Alfalfa site (Appendix Figure 1) and no hardpans of caliche layers were observed in the field. The uniform distribution of the carbonates suggests that formation of carbonates occurred at all depths with similar rates, without significant accumulation (or redistribution) at depth as observed in the Jornada site. The Alfalfa soil profile changes from clayey loam soils near the surface to more sandy soils at the bottom of the soil pit (Cox, 2012), and thus the increased drainage due to the change of soil texture may limit the formation of carbonates at depth at this site.

5.2.2. Ages of pedogenic carbonates

Both isotopic dating techniques and petrographic observations have become standardized techniques for dating pedogenic carbonates (e.g., Amundson et al., 1994; Ludwig and Paces, 2002; Sharp et al., 2003; Candy et al., 2005; Pustovoyotov et al., 2007). In old soils, when pedogenic carbonates form continuous coatings on detrital clasts (Selleck and Baran, 2003), the calcite rind thickness is found to be positively correlated with soil age, even though climate conditions can differ among sites (Amoroso,

2006). Ages of these carbonates were used to establish relative ages of soil genesis and the geomorphic surface. Previously, ages of pedogenic carbonates within the Jornada basin have been constrained using radiocarbon dating through the Desert Project (Gile et al., 1981). Radiocarbon ages are useful for dating materials that are younger than 30 ka. Many sites within the Desert Project had surface ages beyond the dating limit of the ¹⁴C technique in the late Pleistocene or older soils that are common in the Jornada basin. The U-series technique can date much older samples up to ~600 ka. In this study, U-Th isotope disequilibrium systems dated pedogenic carbonates that are as old as 100ka, as discussed below.

Ages of pedogenic carbonates show systematic differences for soils between the Jornada and Alfalfa sites (Fig. 5). The hard-pan caliche samples from the bottom of the Jornada soil pits have the oldest carbonate ages, 117 ± 26 ka and 100 ± 40 ka, for samples from pits JPT1 and JPT2 respectively. This region is characterized as the Jornada I geomorphic surface and its geomorphic age is estimated at 500 – 700ka (Giles et al., 1981). The carbonate ages are much younger than the geomorphic surfaces. These carbonate samples were obtained at 40-50cm depth from the upper most boundary of the thick hard-pan caliche layer. Such observations suggest that the formation of pedogenic carbonates began to accumulate at least ~100 kyrs ago at this site. As such, much older carbonates are expected deeper in the caliche layer. These ages are consistent with the conceptual model that caliche layers generally grow upward and become younger towards the land surface, especially when thick hardpan caliche layers form an impermeable layer that prevents infiltration of soil water to depth. Indeed, much younger pedogenic carbonates are observed in the shallow soil columns (0-50cm depths) at Jornada, with ages ranging from 15 ± 7 ka and 50 ± 21 ka. The shallowest soil samples at JPT1 and JPT2 had relatively large uncertainties in carbonate ages, probably due to the contribution of carbonate from multiple non-pedogenic sources such as dust (see Section 4.4). For Jornada soils, the carbonate ages tended to decrease slightly towards surface but the majority of the ages remained relatively constant with depth. We posit that the formation of the hardpan caliche layer plays an important role in limiting water penetration to deeper soils, and thereby promotes carbonate formations at shallower depths. Indeed, the continuous accumulation of calcite clogs soil pores and can make caliche relatively impermeable to water. Consequently, soil water

may pond on top of the caliche layer, keeping dissolved Ca in shallow soils, which has thereby promoted the accumulation of pedogenic calcite for the last 100 kyr. This is consistent with the laminar texture observed at Jornada on Stage IV pedogenic carbonates (Gile et al., 1966; Gile and Grossman, 1979; Gile et al., 1981; Machette, 1985; Capo and Chadwick, 1999; Chiquet et al., 1999; Monger and Gallegos, 2000; Naiman et al., 2000; Deutz et al., 2002). In this study, no apparent laminar texture was observed in the collected caliche samples, probably due to the fact that these caliche samples were collected from the upper most layer of Stage IV carbonates.

Compared to Jornada soils, pedogenic carbonates in Alfalfa soils are much younger, with Useries ages between 2.2 ± 1.7 ka to 22.2 ± 8.1 ka. Consistent with their younger ages, the pedogenic carbonates are present as films and filaments in the soil matrix, which are typical of the early stages of carbonate development (e.g. Birkeland et al., 1991). The U-series isotope ratios of the bulk soils indicate modification through the addition of U from irrigation water and/or fertilizers. Consequently, irrigation loading of Ca²⁺ and bicarbonate to soils leads to new calcite precipitation through Reaction 1. Indeed, the Rio Grande and local groundwater water used for irrigation in this region is near saturation with calcite and becomes more super-saturated after extensive evapotranspiration (Cox, 2012; Cox et al., 2017). Soils developed on the Rio Grande floodplains in the late Holocene have been intensively cultivated for the last 100 years, explaining why irrigation-induced pedogenic carbonates are extremely young (<100 years old). The continuous addition of irrigation-induced calcite lowers the average age of the bulk pedogenic carbonates over time. Thus, we suggest that the young carbonate ages (e.g. $\sim 2.2 \pm 1.7$ ka) observed at the Alfalfa soils reflect mixing of naturally formed but older carbonates with younger and irrigation-induced carbonates. Different to the Jornada site, the transition from clay loam to sandy soil texture at 60 cm at the Alfalfa site allows for the movement of water and its solutes into much deeper soils and thus accumulation of salts and secondary calcite is not limited to shallow soils.

5.2.3. Pedogenic carbonate accumulation rates

The total amount of pedogenic carbonate accumulated at each site (M; g m⁻²) can be quantified following integration over the entire soil profile sampled:

$$M = \sum_{i} (\rho_i l_i C_i)$$
 Eq. (1)

where ρ is soil bulk density (g cm⁻³), 1 is the soil sampling interval (cm), and C is the pedogenic carbonate content (calculated from SIC; g g⁻¹) at depth interval *i*. The bulk density data used for calculating *M* were from Cox (2012) for the Alfalfa site and Monger et al. (2009) for the Jornada site. The average formation age of pedogenic carbonate for each site (t, yr) is the U-series age weighted by the mass of pedogenic carbonate at each depth, estimated as:

$$t = \sum_{i} (\rho_i l_i C_i t_i) / \sum_{i} (\rho_i l_i C_i) \quad \text{Eq. (2)}$$

Accordingly, the average age of pedogenic carbonate is $\sim 7.3 \pm 5.0$ ka at the Alfalfa site, $\sim 28 \pm 11$ ka at JPT1 and 34 ± 14 ka at JRT2 (the age uncertainty is the average uncertainty of each profile). The accumulation rate of pedogenic carbonate for a given site is thus calculated as (gCaCO₃ m⁻² yr⁻¹):

$$R = \frac{M}{t}$$
 Eq. (3)

Accordingly, pedogenic carbonate accumulation rates were estimated at 9 ± 6 g CaCO₃ m⁻² yr⁻¹ at the Alfalfa site, 3.5 ± 1.5 g CaCO₃ m⁻² yr⁻¹ at JPT1 and 2.5 ± 1.0 g CaCO₃ m⁻² yr⁻¹ at JPT2 on the Jornada. According to Eq. (3), the uncertainty of R is derived mainly from errors in t. Natural accumulation rates of pedogenic carbonates were estimated to range from <0.1 to 15 gCaCO₃ m⁻² yr⁻¹ in New Mexico and Utah (Gile et al., 1981; Machette, 1985; Monger and Gallegos, 2000), 1.0 to 3.5 gCaCO₃ m⁻² yr⁻¹ in the Mojave Desert (Schlesinger, 1985), and 8.3 to 11 gCaCO₃ m⁻² yr⁻¹ in Saskatchewan, Canada (Eghbal and Southard, 1993; Landi et al., 2003). The rates estimated at Jornada (2.5 to 3.5 g CaCO₃ m⁻² yr⁻¹) are within the range estimates of these other non-irrigated systems.

If considering the uncertainties, the accumulation rate of CaCO₃ at the Alfalfa site $(9 \pm 6 \text{ g})$ CaCO₃ m⁻² yr⁻¹) is similar to those documented for the natural Jornada sites $(2.5 \pm 1.0 \text{ to } 3.5 \pm 1.5 \text{ g})$ CaCO₃ m⁻² vr⁻¹). However, the calculated rate represents a minimum value for the Alfalfa soils, given that soils below 70 cm were not sampled. Indeed, characterization of soil salinity for a 3-m-deep profile at the Alfalfa site (only 2 m away from the soil profile of this study) revealed that most salt built up occurred ~2m depth below the land surface, where soil texture changed from being loamy at surface to silty at depth (unpublished data). This suggests that carbonate accumulation rates at Alfalfa should be much higher than 9 ± 6 g CaCO₃ m⁻² vr⁻¹. Estimates using irrigation rates and water chemistry at the same Alfalfa site give accumulation rates of 2.5 mole CaCO₃ m⁻² yr⁻¹ or 250 g CaCO₃ m⁻² yr⁻¹ (Cox et al., 2017), which represent a maximum amount of calcite precipitation from irrigation. This latter exercise suggests that the accumulation rate of secondary calcite is much higher at the Alfalfa site compared to the Jornada site, and that pedogenic accumulation rates are accelerated by agricultural activities such as flood irrigation (discussed further in 5.3.3 below). This comparison is focused on the same depth range from the land surface for the natural and agricultural sites (top 40-50 cm). For the natural site, this rate is probably a good estimate of active carbonate formation for the entire soil profile, because the underlying caliche is closed to water penetration as discussed above.

5.3. Calcium sources in dryland irrigated and non-irrigated soils

According to Reaction 1, the precipitation of pedogenic carbonate is controlled by the availability of Ca²⁺ and dissolved inorganic carbon. Given that most soils are covered by vegetation, even in dryland areas, and thus are in CO₂-open systems, soils have unlimited supply of dissolved inorganic carbon. The amounts and rates of pedogenic carbonate formation in soils of the US Southwest vary greatly and are mostly controlled by Ca²⁺ input, precipitation, and soil age (Gile et al., 1981; Machette, 1985). Below, we compile and estimate the ranges of Ca fluxes from potential sources in natural and agricultural soils in the US southwest. Most of the data for natural environments were derived through the USDA Desert Soil-

Geomorphology Project (Monger and Gallego, 2010). Major sources of Ca²⁺ in natural soils include insitu chemical weathering of soil minerals and atmospheric additions (dry and wet deposition). The emphasis for this study will be comparing these natural loads with those from agricultural practices (i.e., irrigation).

5.3.1. In-situ silicate and carbonate weathering in soils

Alfalfa and Jornada soils have developed on parent material with extremely low carbonate contents. Rio Grande ancestral deposits (Camp Rice Formation), parent sediments of the Alfalfa soils, contain only up to 1% CaCO₃ (Gile et al., 1981). The Jornada soils have also developed on the Camp Rice Formation that are influenced by rhyolitic alluvium from the nearby mountains. The volcanic alluvial deposits contain approximately 0.16 to 3.95% CaO (Monger and Gallegos, 2000) (Table 2). Measurable CaO is observed in all three soil profiles, mainly in the form of pedogenic calcite, with some addition from silicate minerals such as plagioclase as observed by XRD. Evaporite minerals such as gypsum are also present at trace levels as measured through soil-water extraction methods, but no phases were detected by XRD (Cox et al., 2017). In this study, gypsum is considered as a secondary mineral with Ca sourced from dust or irrigation water as discussed below. Hence gypsum is not considered a separate Ca input flux here. Silicate weathering in dryland soils is expected to be extremely slow, due to both the limited amount of rainfall and the relatively neutral soil water pH. Indeed, the rates of plagioclase dissolution are lower for the JPT1 soils, where less than 10% of CaO is derived from silicate minerals and the dissolution kinetics is further limited by mineral surfaces (Fig. 3). Similarly, in consideration of the mass balance and isotope signature of Sr, previous studies have also identified the dissolution of silicate rocks as a minor contributor to the overall loading of Ca in pedogenic carbonates of the US Southwest (Machette, 1985; Capo and Chadwick, 1999).

5.3.2. Atmospheric depositions (dust and rainfall)

Contributions of atmospheric deposition soil carbonates have been vigorously investigated (e.g., Gile et al., 1961; Grossman et al., 1995; Chiquet et al., 1999; Chiquet et al., 2000) and several studies have identified that Ca in pedogenic carbonates in dryland soils of the US southwest is mainly dust-derived (Gile et al., 1981; Capo and Chadwick, 1999; Naiman et al., 2000). A 10-year survey through the Desert Project in New Mexico trapped and analyzed dust samples, and estimated that dust loaded calcite at an average rate of 0.3 gCaCO₃ m⁻² yr⁻¹ (range: 0.2 to 0.4) and other types of water leachable Ca at an equivalent rate of 0.14 gCaCO₃ m⁻² yr⁻¹ (range: 0.10-0.17) (Gile and Grossman, 1979; Gile et al., 1981; Monger and Gallegos, 2000). More build-up of pedogenic carbonates in soils has been also associated with Ca²⁺ dissolved in rainfall (Gile and Grossman, 1979; Capo and Chadwick, 1999; Monger and Gallegos, 2000). It has been estimated that Ca is added to soils in US Southwest via wet deposition at an equivalent of 1.5 gCaCO₃ m⁻² yr⁻¹ (Monger and Gallegos, 2000), making the total Ca input from atmospheric deposition 1.9 gCaCO₃ m⁻² yr⁻¹. The above estimates assume that carbon was made available by root respiration and microbial activity and was unlimited (Gile et al., 1979).

5.3.3. Land management practices

With limited rainfall, flood irrigation is essential for successful cultivated agriculture in the US Southwest, including the Alfalfa site near El Paso, TX. Every year from April to October, the field is flood irrigated every two to three weeks with standing water from the Rio Grande River. The salinity of river water near the study site but slightly downstream ranges from 700 to 2000 mg/l with calcite saturation index at ~1.2 (Cox, 2012). Approximately 1.5 m of this water are used for flood-irrigating the alfalfa farm every year, loading dissolved Ca at an equivalent rate of ~250 gCaCO₃ m⁻² yr⁻¹ (Cox, 2012; Cox et al., 2017). The irrigation water becomes concentrated through evapotranspiration. As a result, evaporite salts precipitate, leading to elevated soil salinity and sodicity (Cox, 2012; Cox et al., 2017). Indeed, calcite is observed throughout the soil profile at the Alfalfa site and other agricultural soils of the El Paso region, and halite and gypsum might be even present (Cox, 2012). Importantly, the fluxes estimated above should be

considered as a maximum amount of Ca²⁺ input from irrigation, as some losses of Ca occur through drainage into agricultural canals and groundwater recharge (Cox, 2012).

In addition to irrigation, N and P fertilizers such as mono-ammonium phosphate are commonly used to increase crop yields in the region. To mitigate sodicity and improve soil structure, gypsum and other Ca-bearing soluble minerals are usually supplied to the agricultural fields, where Ca²⁺ replaces Na⁺ in soils as a result. Such practices are especially important for loamy to clayey soils because these relatively impermeable soils tend to accumulate more salts and lead to more sodic conditions. At the Alfalfa site, fertilizers were commonly applied but no Ca minerals have been added in the last five years and no historical records of Ca applications are available beyond this time period. Future work on Sr and U isotopes is needed to better trace the sources of Ca in pedogenic carbonates and to evaluate the relative importance of fertilizers and Ca-minerals in the overall Ca budgets of agricultural soils (*sensu* Garcia, 2017).

5.3.4. Summary of Calcium Sources

As discussed above, major Ca sources for pedogenic carbonates were identified and their magnitudes were compiled based on literature and our previous studies (Cox, 2012; Cox et al., 2017). These bulk estimates suggest that the formation of pedogenic carbonates in natural fields is mainly driven by loading of Ca in dust and rainfall (Capo and Chadwick, 1999). The annual loading from atmospheric inputs (10 years average at 1.9 gCaCO₃ m⁻² yr⁻¹) is similar to the formation rate of pedogenic carbonate at the Jornada (2.5 to 3.5 gCaCO₃ m⁻² yr⁻¹ for up to 100 Ka). In contrast, the Ca (and DIC) fluxes from agricultural practices were much larger, leading to calcite precipitation at much faster rates. This is consistent with the relatively higher formation rates observed at the Alfalfa site (see Section 5.2.3).

5.4. Implications of dryland irrigation for global carbon cycles

Our study highlights the importance of land use change and irrigated agriculture on pedogenic carbonate formations in the US Southwest and possibly elsewhere in drylands. Irrigation is an important

land management practice in these drylands and its impact on pedogenic carbonate formation is not well constrained because most changes are gradual and can only be observed after a long time period following sustained cultivation (Suarez, 2000). Depending on the chemistry of irrigation water and the amount of water leached to deeper soils, irrigation can either cause accumulation or dissolution of pedogenic carbonates (Sanderman, 2012; Suarez, 2000). In natural soil systems, calcium generally limits the formation of secondary calcite whereas under cultivation, significant amounts of Ca can be loaded through irrigation. Indeed, irrigation water supplies soluble cations (such as Ca²⁺) that can foster pedogenic carbonate formation (Lal and Kimble, 2000; Sanderman, 2012). Cox et al. (2017) studied agricultural soils under cultivation with three major crop species near in El Paso, TX (alfalfa, pecan, and cotton) and reported salt buildup such as pedogenic carbonates in these agricultural fields, especially on fine-grained soils with low permeability. Soluble evaporite minerals such as halite and gypsum were also observed in soils with high salinity and sodicity. Thus, it is reasonable to assume that deposition rates of pedogenic carbonates are accelerated in irrigated agricultural lands along the Rio Grande valley, beyond the alfalfa site studied here.

Irrigation also increases soil CO_2 by precipitating carbonates through Rxn (1) and increasing biological activity (Suarez, 2000; Sanderman, 2012), thus modifying soil-atmosphere carbon fluxes. To date, representation of the potential shift in land-atmosphere CO_2 exchange associated with dryland agriculture has been poorly recognized and models forecasting the future state of the Earth System do not include such dynamics. Human land use changes and activities such as irrigation, application of synthetic fertilizers, and afforestation all impact soil organic carbon pools (Lal and Kimble., 2000b). How these changes and activities contribute to soil inorganic carbon is not well documented and warrants future study. Indeed, few studies have quantified the production and emission of CO_2 during the development of pedogenic carbonates in agricultural drylands (e.g., Amundson and Lund, 1987; Lal and Kimble, 2000; Wohlfahrt et al., 2008; Xie et al., 2009; Liu et al., 2012). One modeling study estimated that approximately 2.2 TgC yr⁻¹ (1Tg = 10^{12} g) were released to the atmosphere from approximately 16 million ha of irrigated dryland fields in the western US (Suarez, 2000), which is equivalent to a release of soil CO_2 to the atmosphere at 14 gC m⁻² yr⁻¹. The stoichiometry of Reaction (1) implies 14 gC m⁻² yr⁻¹ was also accumulated

in soils as peodgenic carbonates, which is one to two orders of magnitude higher than natural pedogenic carbonate accumulation rates (Eghbal and Southard, 1993; Landi et al., 2003).

Our study directly compared natural and agricultural landscapes along the Rio Grande valley and observed, even with large uncertainties in carbonate ages, higher accumulation rates of pedogenic carbonates in agricultural fields. The higher calcite accumulation rates observed in Alfalfa soils also point to measurable CO₂ fluxes from agricultural soils to atmosphere. Furthermore, dryland area is expanding and already covers more than 40% of the terrestrial land surface on Earth. Drylands host more than two billion people, with most living in developing countries (Grace et al., 2006; Wang et al., 2012). The combined increase in food demand and desertification has converted 4% of natural dryland to irrigated agriculture coverage (UNCCD, 2000). These findings suggest dryland agriculture has the potential to significantly alter land-atmosphere CO₂ flux over a large area of the Earth's surface.

6. Conclusions

Pedogenic carbonates, are an important component of the global carbon cycle, are ubiquitous in dryland soils. Many studies have studied the sources, quantities, formation rates and mechanisms of these secondary carbonates in natural settings but few have focused on agricultural systems. In this study, calcium oxides and soil carbon concentration, mineralogy and U-series isotopes were investigated concomitantly at an irrigated (Alfalfa field) and a non-irrigated (Jornada) site in the US Southwest to compare and contrast the pedogenic carbonate inventory, age, and formation rate. U-series dating technique indicates younger pedogenic carbonates at the irrigated Alfalfa site compared to carbonates at the non-irrigated Jornada site. However, pedogenic carbonate formation rates at the Alfalfa site were higher compared to those at the Jornada soils. These elevated formation rates were supported by high fluxes of Ca and carbon induced by flood irrigation in the agricultural fields. These findings suggest dryland agriculture has the potential to significantly alter land-atmosphere CO₂ flux and long-term dryland-atmosphere dynamics over a large area of the Earth's surface.

7. Acknowledgements

We thank the field and laboratory assistance from Christine Cox, David Borrok, and Girisha Ganjegunte, and financial support from Startup funds for LJ and LM at UTEP. SN and LM acknowledge partial financial support for U-series analysis in Rio Grande water samples from NSF EAR 1349091, NSF HRD 1242122, and NSF DEB/LTER 0080412. Associate Editor and two anonymous reviewers are acknowledged for their thorough and constructive comments that improved the quality of the manuscript.

REFERENCES

- Amoroso, L. (2006) Age calibration of carbonate rind thickness in Late Pleistocene soils for surficial deposit age estimation, Southwest USA. *Quaternary Research* **65**, 172-178.
- Amundson, R.G., and Lund, L.J. (1987) The stable isotope chemistry of a native and irrigated Typic Natrargid in the San-Joaquin Valley of California. *Soil Science Society of America Journal* 51, (3), 761-67.
- Amundson, R.G., Wang, Y., Chadwick, O.A., Trumbore, S., McFadden, L., McDonald, E., Wells, S. and Deniro, M. (1994) Factors and processes governing the C-14 content of carbonate in desert soils. *Earth and Planetary Science Letters* 125, 385-402.
- Andersen, M.B. et al., 2008. High-precision U-series measurements of more than 500,000 year old fossil corals. Earth and Planetary Science Letters, 265(1-2): 229-245.
 - Andrews JA, Schlesinger WH (2001) Soil CO₂ dynamics, acidification, and chemical weathering in a temperate forest with experiment CO₂ enrichment. Global Biogeochemical Cycles 15:149-162.
- Bergametti, G. and Gillette, D.A., 2010. Aeolian sediment fluxes measured over various plant/soil complexes in the Chihuahuan desert. Journal of Geophysical Research-Earth Surface, 115.
- Birkeland, P.W., Machette, M.N., and Haller, K.M. (1991). Soils as a tool for applied Quaternary geology [Utah Geological and Mineral Survey Misc. Pub. 91-3]. Salt Lake City: Utah Department of Natural Resources.
- Bischoff, J.L. and Fitzpatrick, J.A., 1991. U-Series Dating of Impure Carbonates an Isochron Technique Using Total-Sample Dissolution. Geochimica Et Cosmochimica Acta, 55(2): 543-554.
- Candy, I., Black, S and Sellword, B.W. (2005) U-series isochron dating of immature and mature calcretes as a basis for constructing Quaternary landform chronologies for the Sorbas basin, southern Spain. Quaternary Research 64, 100-111.
- Capo, R.C. and Chadwick, O.A., 1999. Sources of strontium and calcium in desert soil and calcrete. Earth and Planetary Science Letters, 170(1-2): 61-72.
- Cerling, T.E., 1984. The Stable Isotopic Composition of Modern Soil Carbonate and Its Relationship to Climate. Earth and Planetary Science Letters, 71(2): 229-240.
 - Cerling, T.E., Quade, J., Wang, Y. and Bowman, J.R. (1989) Carbon isotopes in soils and palaeosols as paleoecologic indicators. Nature 341: 138-139.
- Chabaux, F., Bourdon, B., and Riotte, J. (2008), U-series geochemistry in weathering profiles, river waters and lakes. Radioactivity in the Environment 13, 49-104.
- Chabaux, F., Riotte, J., and Dequincey., O. (2003), U-Th-Ra fractionation during weathering and river transport. Reviews in Mineralogy and Geochemistry 52, 533–576.
- Chadwick, O.A., Sowers, J.M. and Amundson, R.G. (1989) Morphology of calcite crystals in clast coatings from four soils in the Mojave Desert region. *Soil Sci. Soc. Am. J.* 52, 211-219 (1988).
- Cheng, H., Edwards, R.L., Hoff, J., Gallup, C.D., Richards, D.A., Asmerom, Y. (2000), The half-lives of uranium-234 and thorium-230. Chem. Geol. 169, 17-33.
- Cheng, H., Edwards, R.L., Sinha, S., Spötl, C., Yi, L., Chen, S., Kelly, M., Kathayat, G., Wang, X., Li, X., Kong, X., Wang, Y., Ning, Y., and Zhang, H. (2016). The Asian monsoon over the past 640,000 years and ice age terminations. Nature 354, 640-646.
- Chiquet, A., Colin, F., Hamelin, B., Michard, A and Nahon, D. (2000) Chemical mass balance of calcrete genesis on the Toledo granite (Spain). Chemical Geology 170, 19-35.
- Chiquet, A., Michard, A., Nahon, D. and Hamelin, B., 1999. Atmospheric input vs insitu weathering in the genesis of calcretes: An Sr isotope study at Galvez (Central Spain). Geochemica et Coscochimica Acta 63: 311-323.
- Cox, C.L., 2012. Evaluation of soil sustainability along the Rio Grande in West Texas: changes in salt loading and organic nutrients due to farming practices, University of Texas at El Paso, El Paso, TX, 48 pp.

- Cox, C.L., Jin, L., Ganjegunte, G., Borrok, D., Lougheed, V., and Ma, L. (2017) Soil quality changes due to flood irrigation in agricultural fields along the Rio Grande in western Texas. To be submitted to Applied Geochemistry.
- D'Odorico, P., Bhattachan, A., Davis, K., Ravi, S., and Runyan, C. (2012) Global desertification: drivers and feedbacks, Adv. Water Re-sour., doi:10.1016/j.advwatres.2012.01.013.
- Deutz, P., Montanez, I.P. and Monger, C.H., 2002. Morphology and Stable and Radiogenic Isotope Composition of Pedogenic Carbonates in Late Quaternary Relict Soils, New Mexico, U.S.A.: An Integrated Record of Pedogenic Overprinting. Journal of Sedimentary Research, 72(6): 809-822.
- Dickin, A.P. (1995). Radiogenic Isotope Geology. Cambridge University Press, Cambridge. 490.
- Dosseto, A., Turner, S.P., and Chappell, J. (2008), The evolution of weathering profiles through time: New insights from uranium-series isotopes. Earth and Planetary Science Letters 274, 359–371.
- Dregne, H.E. (1991) Human activities and soil degradation." Semiarid Lands and Deserts: Soil Resource and Reclamation, 335-360.
- Edwards, R.L., Gallup, C.D. and Cheng, H., 2003. Uranium-series Dating of Marine and Lacustrine Carbonates. Reviews in Mineralogy and Geochemistry, 52: 363-405.
- Eghbal, M.K. and Southard, R.J. (1993) Stratigraphy and genesis of Durorthids and Haplargids on dissected alluvial fans, western Mojave Desert, California. *Geoderma* 59, 151-174.
- Egli, M., and Fitze, P. (2001) Quantitative aspects of carbonate leaching of soils with differing ages and climates. *Catena* 46, 35-62.
- Ellis, S.R., Levings, G.W., Carter, L.F., Richey, S.F., and Radell, M.J., 1993, Rio Grande Valley, Colorado, New Mexico, and Texas. Water Resources Bulletin 29: 617–646.
- Entry, J.A., Sojka, R.E. and Shewmaker, G.E., 2004. Irrigation increases inorganic carbon in agricultural soils. Environmental Management, 33: S309-S317.
- Eswaran, H. et al., 2000. Global carbon sinks. In: J.M.K. R. Lal and B.A. Stewart. (Editors), Global Climate Change and Pedogenic Carbonates. CRC/Lewis Press, Boca Raton, Fla, pp. 15–26.
- Feldman, C., 1983. Behavior of Trace Refractory Minerals in the Lithium Metaborate Fusion-Acid Dissolution Procedure. Analytical Chemistry, 55(14): 2451-2453.
- Ghassemi, F., Jakeman, A.J. and Nix, H.A. (1995). Salinisation of Land and Water Resources: Human Causes, Extent, Management and Case Studies, University of New South Wales Press, Sydney and CAB International, Wallingford.
- Gibbens, R.P., McNeely, R.P., Havstad, K.M., Beck, R.F. and Nolen, B., 2005. Vegetation changes in the Jornada Basin from 1858 to 1998. Journal of Arid Environments, 61(4): 651-668.
- Gile, L.H. (1961). A classification of ca horizons in the soils of a desert region, Dona Ana County, New Mexico. *Soil Science Society of America Proceedings* 25, 52–61.
- Gile, L.H. and Grossman, R.B. (1979) The Desert Project soil monograph: Soils and landscapes of a desert region astride the Rio Grande Valley near Las Cruces, New Mexico. Lincoln, NE: U.S. Department of Agriculture, Soil Conservation Service.
- Gile, L.H. and Grossman, R.B., 1979. The Desert Project soil monograph. US Government Printing Office, Washington, DC.
- Gile, L.H., Hawley, J.W. and Grossman, R.B., 1981. Soils and geomorphology in the Basin and Range area of Southern New Mexico: Guidebook to the Desert Project. New Mexico Bureau of Mines and Mineral Resources., Socorro, NM, 222 pp.
- Gile, L.H., Peterson, F.F. and Grossman, R.B., 1966. Morphological and genetic sequences of carbonate accumulation in desert soils. Soil Science 101: 347–360.
- Gillette, D. and Monger, H.C., 2006. Eolian processes on the Jornada Basin. In: K.M. Havstad, L.F. Huenneke and W.H. Schlesinger (Editors), Structure and Function of a Chihuahuan Desert Ecosystem. The Long-term Ecological Research Network Series. Oxford University Press, New York, pp. 189-210.
- Grace, J., Jose, J.S., Meir, P., Miranda, H.S., and Montes, R.A. (2006) Productivity and carbon fluxes of tropical savannas, *J. Biogeogr.*, 33, 387–400.
- Grossman, R. B., Ahrens, R. J., Gile, L. H., Montoya, C. E., & Chadwick, O. A. (1995). Areal evaluation

- of organic and carbonate carbon in a desert area of southern New Mexico. In R. Lal, J. Kimble, E. Levine, & B. A. Steward (Eds.), Soils and global change (pp. 81–92). Boca Raton, FL: CRC Press, Inc.
- Gutschick, V.P., Snyder, K.A. 2006. Water and Energy Balances within the Jornada Basin. In "Structure and Function of Chihuahuan Desert Ecosystem, The Jornada Basin Long-Term Ecological Research Site" Edited by: Kris Havstad, Laura F. Huenneke, William H. Schlesinger.
- Hawley, J.W. and Kennedy, J.F., 2004. Creation of a Digital Hydrogeologic Framework Model of the Mesilla Basin and Southern del Muerto Basin, New Mexico Water Resources Research Institute Technical, Las Cruces, New Mexico.
- Hirmas, D.R., Amrhein, C., Graham, R.C. (2010) Spatial and process-based modeling of soil inorganic carbon storage in an arid piedmont. *Geoderm* 154, 486-494.
- Hogan, F.M., Phillips, F.M., Mills, S.K., Hendrickx, J.M.H., Ruiz, J., Chesley, J.T., Asmerom, Y. (2007) Geologic origins of salinization in semi-arid river: the role of sedimentary basin brines. *Geology* 35, 1063–1066.
- Hutchison, W.R. (2006) Groundwater management in El Paso, Texas. Dissertation.com, Boca Raton, FL. Ivanovich, M. and Harmon, R.S., 1992. Uranium-series disequilibrium: Applications to earth, marine, and environmental sciences. Clarendon Press, Oxford University Press.
- Junge, C.E. and Werby, R.T., 1958. The Concentration of Chloride, Sodium, Potassium, Calcium, and Sulfate in Rain Water Over the United States. Journal of Meteorology, 15(5): 417-425.
- Keller, G.R., Morgan, P. and Seager, W.R., 1990. Crustal Structure, Gravity-Anomalies and Heat-Flow in the Southern Rio-Grande Rift and their Relationship to Extensional Tectonics. Tectonophysics, 174(1-2): 21-37.
- Kraimer, R.A. and Monger, H.C. (2009) Carbon isotopic subsets of soil carbonate- A particle size comparison of limestone and igneous parent materials. *Geoderma* 150, 1-9.
- Ku, T.L., Bull, W.B., S.T., F. and Knauss, K.G., 1979. Th²³⁰-U²³⁴ dating of pedogenic carbonates in gravelly desert soils of Vidal Valley, southeastern California. Geological Society of America Bulletin, 90(11): 1063-1073.
- Kummerer, K, Held, M. and Pimentel, D. (2010) Sustainable use of soils and time. *Journal of Soil and Water Conservation* 65, 141-149.
- Kuzyakov, Y. and Domanski, G. (2000) Carbon input by plants into soil. Review. J. Plant Nutr. Soil Sci. 163, 421-431.
- Lahann, R.W. (1978) A chemical model for calcite crystal growth and morphology control. *J. Sedi. Petrol.* 48, 337-344.
- Lal, R. and Kimble, J.M., 2000a. Inorganic carbon and the global C cycle: Research and development priorities. Global Climate Change and Pedogenic Carbonates. CRC/Lewis Publishers, Boca Raton, Florida, 291-302 pp.
- Lal, R. and Kimble, J.M., 2000b. Pedogenic carbonates and the global carbon cycle. In: R. Lal, J.M. Kimble, H. Eswaran and B.A. Stewart (Editors), Global climate change and pedogenic carbonates. Lewis Publishers, Boca Raton, pp. 1-14.
- Landi, A., Mermut, A.R., Anderson, D.W. (2003) Origin and rate of pedogenic carbonate accumulation in Saskatchewan soils, Canada. *Geoderma* 117, 143-156.
- Langmuir, D. and Herman, J.S., 1980. The Mobility of Thorium in Natural-Waters at Low-Temperatures. Geochimica Et Cosmochimica Acta, 44(11): 1753-1766.
 - Laudicina, V.A., Scalenghe, R., Piscoiotta, A., Parello, F., Dazzi, C. (2013) Pedogenic carbonates and carbon pools in gypsiferous soils of a semiarid Mediterranean environment in south Italy. *Geoderma* 192, 31-38.
 - Liu, R., Li, Y, Wang, Q.X. (2012) Variations in water and CO₂ fluxes over a saline desert in western China. *Hydrological Process* 26, 513–522.
- Ludwig, K.R. and Paces, J.B. (2002) U-series dating of pedogenic silica and carbonate, Crater Flat. Nevada. *Geochim. Cosmochim. Acta* 66, 487–506.

- Ludwig, K.R., 2003. Mathematical-statistical treatment of data nd errors for Th-230/U geochronology. Uranium-Series Geochemistry, Reviews in Minerology and Geochemistry, 52: 631-656.
- Luo, S.D. and Ku, T.L., 1991. U-Series Isochron Dating A Generalized-Method Employing Total-Sample Dissolution. Geochimica Et Cosmochimica Acta, 55(2): 555-564.
- Machette, M.N., 1985. Calcic soils of the southwestern United States. Geological Society of America 203: 1–21.
- Mack, G.H. and James, W.C., 1992. Calcic paleosols of the Plio-Pleistocene Camp Rice and Palomas Formations, southern Rio Grande rift, USA. Sedimentary Geology, 77(1-2): 89-109.
- Mack, G.H., Love, D.W. and Seager, W.R., 1997. Spillover models for axial rivers in regions of continental extension: the Rio Mimbres and Rio Grande in the southern Rio Grande rift, USA. Sedimentology, 44(4): 637-652.
- Marion, G.M. and Schlesinger, W.H. (1994) Quantitative modeling of soil forming process in desert: the CALDEP and CALGYP models. In: Bryant, R.B. and Arnold, R.W. (Eds.), Quantitative modeling of soil forming processes. SSSA special publication 39, 129-145.
 - McFadden, L.D. and Tinsley, J.C. (1985) Rate and depth of pedogenic carbonate accumulation in soils: formation and testing of a compartment model. In (Eds.Weide, D.L.) *Geological Society of America special paper* 203, 23-42.
- Miyamoto, S., 2002. Landscape irrigation with water of elevated salinity: Guide for planners, managers and supervisors. Texas A&M Univ. Agr. Res. Ctr. at El Paso
- Miyamoto, S., 2012. Salinization of Irrigated Urban Soils: A Case Study of El Paso, Texas. 434, Texas A&M University, Texas Water Resources Institute.

 Miyamoto, S., and A. Chacon, 2006. Soil salinity of urban turf areas irrigated with saline water. II. Soil
- Miyamoto, S., and A. Chacon, 2006. Soil salinity of urban turf areas irrigated with saline water. II. Soil factors. Landsc. & Urban Plan. 77:28-38.
- Monger, C.H., Gile, L.H., Hawley, J.W. and Grossman, R.B., 2009. The Desert Project-An Analysis of Aridland Soil-Geomorphologic Processess, New Mexico State University, Las Cruces, NM.
- Monger, H.C. and Gallegos, R.A., 2000. Biotic and abiotic processes and rates of pedogenic carbonate accumulation in the southwestern United States-relationship to atmospheric CO2 sequestration. In Global Climate Change and Pedogenic Carbonates. CRC/Lewis Press, Boca Raton, Fla, 273-289 pp.
 - Monger, H.C. and Martinez-Rios, J.J. (2001). Inorganic carbon sequestration in grazing lands. In R. F. Follett, J. M. Kimble, & R. Lal (Eds.), The potential of U.S. grazing lands to sequester carbon and mitigate the greenhouse effect, 87–118. Boca Raton, FL: Lewis Publishers.
- Monger, H.C., 2006. Regional Setting of the Jornada Basin In: K. Havstad, I.F. Huenneke and W.H. Schlesinger (Editors), Structure and Function of Chihuahuan desert Ecosystem: The Jornada Basin Long-Term Ecological Research Site The Long-Term Ecological Research Network Series. Oxford University Press, pp. 492.
- Monger, H.C., Daugherty, L.A., Lindemann, W.C. and Liddell, C.M., 1991. Microbial Precipitation of Pedogenic Calcite. Geology, 19(10): 997-1000.
- Moore, S.J., Bassett, R.L., Liu, B., Wolf, C.P. and Doremus, D., 2008. Geochemical tracers to evaluate hydrogeologic controls on river salinization. Ground Water, 46(3): 489-501.
- Naiman, Z., Quade, J. and Patchett, P.J., 2000. Isotopic evidence for eolian recycling of pedogenic carbonate and variations in carbonate dust sources throughout the southwest United States. Geochimica Et Cosmochimica Acta, 64(18): 3099-3109.
- Neymark, L.A., 2011. Potential effects of alpha-recoil on uranium-series dating of calcrete. Chemical Geology, 282(3-4): 98-112.
- Ontl, T.A. and Schulte, L.A., 2012. Soil Carbon Storage. Nature Education Knowledge, 3(10): 35.
- Osmond, J.K., May, J.P., and Tanner, W.F. (1970) Age of the Cap Kennedy barrier-and-lagoon complex. *J. Geophys. Res.* 75, 5459-5468.
- Oster, J.L., Ibarra, D.E., Harris, C.R., and Maher, K. (2012) Influence of eolian deposition and rainfall amounts on the U-isotopic composition of soil water and soil minerals. *Geochmica et Cosmochimica Acta* 88, 146-166.

- Oster, J.L., Kitajima, K., Valley, J.W., Rogers, B. and Maher, K. (2017) An evaluation of paired δ¹⁸O and (²³⁴U/²³⁸U)₀ in opal as a tool for paleoclimate reconstruction in semi-arid environments. *Geochemical Geology* 449, 236-252.
- Paces, J.B., and Whelan, J.F. (2012) The paleohydrology of unsaturated and saturated zones at Yucca Mountain, Nevada, and vicinity, in Stuckless, J.S., ed., Hydrology and Geochemistry of Yucca Mountain and Vicinity, Southern Nevada and California: Geological Society of America Memoir 209, p. 219-276, doi:10.1130/2012.1209(05).
 - Phillips, F.M., Hogan, J., Mills, S. and Hendrickx, M.H. (2003) Environmental tracers applied to quantify causes of salinity in arid-region rivers: Preliminary results from the Rio Grande, southwestern USA. In Alsharha, A.S. and Wood, W.W. Eds., Water resources perspective: evaluation, management, and policy: Developments in water science, V50, Amsterdam, Elsevier Science, 327-334.
 - Pimentel, D., Harvey, C., Resosudarmo, P., Sinclair, K., Kurz, D., McNair, M., Crist, S., Shpritz, L., Fitton, L, Saffouri, R. and Blair, R. (1995) Environmental and Economic costs of soil erosion and conservation benefits. *Science* 267 (5201), 1117-1123.
- Pustovoytov, K., Schmidt, K. and Taubald, H. (2007) Evidence for Holocene environmental changes in the northern fertile Crescent provided by pedogenic carbonate coatings. Quaternary Research 67, 315-327.
 - Quade, J., Cerling, T.E. and Bowman, J.R. (1989) Systematic variations in the carbon and oxygen isotopic composition of pedogenic carbonate along elevation transects in the southern Great Basin, United States. *Geological Society of America Bulletin* 101, 464-375.
- Rosholt, J.N., (1976), 230Th/234U dating of travertine and caliche rinds, GSA abstr. Prog. 8, 1076. Royer, D.L. (1999) Depth to pedogenic carbonate horizon as a paleoprecipitation indicator? *Geology* 27, 1123-1126.
- Sanderman, J., 2012. Can management induced changes in the carbonate system drive soil carbon sequestration? A review with particular focus on Australia. Agriculture, Ecosystems and Environment, 155: 70-77.
 - Schlesinger, W.H. (1982) Carbon storage in the caliche of arid soils: a case study from Arizona. *Soil Science* 133, 247-255.
 - Schlesinger, W.H. (1985) The formation of caliche in soils of Mojave Desert, California. *Geochim. Cosmochim. Acta* 49, 57-66.
 - Schlesinger, W.H. (2000) Carbon sequestration in soils: some cautions amidst optimism. *Agriculture, Ecosystems and Environment* 82, 121-127.
 - Schoups, G., Hopmans, J.W., Young, C.A., Vrugt, J.A., Wanllender, W.W. and Tanji, K.K. (2005) Sustainability of irrigated agriculture in the San Joaquin Valley, California. Proc.
- Seager, W.R., Hawley, J.W., Kottolowski, F.E. and Kelley, S.A., 1987. Geology of east half of Las Cruces and northeast El Paso 1° x 2° sheets, New Mexico, New Mexico, Bureau of Mines & Mineral Resources, Geologic Map 57.
 - Selleck, B. and Baran, J. (2003) Petrology and stable isotope geochemistry of Holocene and Pleistocene calcite cement in kame terrace gravel, central New York State. *Northeastern Geology and Environmental Science* 25(3), 186-196
- Serna-Perez, A., Monger, H.C., Herrick, J.E. and Murray, L., 2006. Carbon dioxide emissions from exhumed petrocalcic horizons. Soil Science Society of America Journal, 70(3): 795-805. Serna-Perez, A., Monger, H.C., Herrick, J.E., and Murray, L. (2006). Carbon dioxide emissions from exhumed petrocalcic horizons. *Soil Science Society of America Journal* 70, 795–805.
- Sharp, W.D., Ludwig, K.R., Chadwick, O.A., Amundson, R. and Glaser, L.L., 2003. Dating fluvial terraces by the ²³⁰Th/U on pedogenic carbonate, Wind River Basin, Wyoming. Quaternary Research 59:139–150.
- Sims K.W.W., Gill, J.B., Dosseto, A., Hoffmann, D.L., Lundstrom, C.C., Williams, R.W., Ball, L., Tollstrup, D., Turner, S., Pyrtulak, J., Glessner, J.G., Standish, J.J. and Elliott, T. (2008): An Inter-Laboratory Assessment of the Thorium Isotopic Composition of Synthetic and Rock Reference Materials. Geostandards and Geoanalytical Research 32(1): 65-91.

- Suarez, D. L. (2000) Impact of Agriculture on CO₂ as Affected by Changes in Inorganic Carbon', in Lal, R., Kimble, J. M., Eswaran, H., and Stewart, B. A. (eds.), Global Climate Change and Pedogenic Carbonates, CRC/Lewis Publishers, Boca Raton, FL, pp. 257–272. Szykiewicz, A., Wither, J., Modelska, M., Borrok, D.M. and Pratt, LM. (2011) Anthropogenic
- Szynkiewicz, A., Borrok, D.M., Skrzypek, G., Rearick, MS. (2015) isotopic studies of the Upper and Middle Rio Grande.Part1-Importance of sulfide weathering in the riverine sulfate budget Chemical Geology 411: 323-335.

sulfate loads in the Rio Grande, New Mexico (USA). Chemical Geology 283, 194-209.

- Vigier, N., Bourdon B., Turner S., and Allegre, C.J. (2001), Erosion timescales derived from U-decay series measurements in rivers. Earth and Planetary Science Letters 193, 485–499.
- Violette, A., Riotte, J., Braun, J., Oliva, P., Marechal, J., Sekhar, M., Jeandel, C., Subramanian, S., Prunier, J., Barbiero, L. and Dupre, B. (2010) Formation and preservation of pedogenic carbonates in Southern Indian, links with paleo-monsoon and pedological conditions: Clues from Sr isotopes, U-Th series and REEs. *Geochimica et Cosmochimica Acta* 74, 7059-7085.
- Vogel, J.S., Southen, J.R., Nelson, D.E. and Brown, T.A. (1984). Performance of catalytically condensed carbon for use in accelerator mass spectrometry. Nuclear Instruments and Methods 223: 289-293.
- Wang, L, D'Odorico, P., Evans, J.P., Eldridge, D.J., McCabe, M.F., Caylor, K.K. and King, E.G. (2012) Dryland ecohydrology and climate change: critical issues and technical advances. *Hydro. Earth Syst. Sci.* 16, 2585-2603.
 - Wohlfahrt, G., Fenstermaker, L.F., Arnone, J.A. (2008) Large annual net ecosystem CO₂ uptake of a Mojave Desert ecosystem. *Global Change Biology* 14, 1475–1487.
 - Xie J., Li Y., Zhai C., Li C., Lan Z. (2009): CO₂ absorption by alkaline soils and its implication to the global carbon cycle. *Environ. Geol.* 56, 953-961.

Figure captions:

Figure 1: Location map showing the two studied sites 1) the Alfalfa field near El Paso, Texas (blue star) and 2) the Jornada Experimental Range (USDA-LTER) in New Mexico (JPT1 and JPT2, red star). The irrigation districts along the Rio Grande valley and the total acreage of the irrigated drylands in this region are also shown for references. EBID: Elephant Butte Irrigation District; EPCWID: El Paso County Water Improvement District; HCCRD: Hudspeth County Conservation and Reclamation District. (www.ebid-nm.org; www.epcwid1.org).

Figure 2: a) Measured XRD calcite/quartz peak intensity ratios (29.42° for calcite and 26.65° for quartz); b) soil inorganic carbon contents (wt. %); c) soil total carbon contents (wt. %); and d) soil organic carbon contents (wt. %) in bulk soil samples from Alfalfa (El Paso, TX) and JPT 1 and JPT 2 (Jornada basin, NM).

Figure 3: a) Soil CaO contents (wt. %) in bulk soil samples from Alfalfa (El Paso, TX) and JPT 1 and JPT 2 (Jornada basin, NM); Relative contribution of soil CaO from calcite vs. silicates in Alfalfa soils (b), JPT1 (c) and JPT2 (d) in Jornada.

Figure 4: Measured U/Th element ratios (a, b), (²³⁴U/²³⁸U) (c, d) and (²³⁰Th/²³⁸U) activity ratios (e, f) in bulk soil samples and caliche samples from Alfalfa (El Paso, TX) and JPT 1 and JPT 2 (Jornada basin, NM).

Figure 5: Calculated U-series ages for pedogenic carbonates in bulk soils from Alfalfa (El Paso, TX) (a) and for pedogenic carbonates in bulk soils (closed symbols) and in hardpan caliche (open symbols) in JPT 1 (b) and JPT 2 (c) (Jornada basin, NM).

Table 1: Mineralogy, carbon contents, major element, U-series isotope concentrations and activity ratios, and calculated U-series isotopes ages for pedogenic carbonates in Alfalfa and Jornada (JPT 1 and JPT 2) samples.

Table 2: Measured (234 U/ 238 U), (230 Th/ 238 U), (232 Th/ 238 U) activity rations for bulk soil and caliche samples, acid leachate and residual, water leachate and residual samples for Alfalfa and Jornada profiles. Correlation coefficients (R^2) for isochron plots (230 Th/ 238 U vs. 232 Th/ 238 U and 234 U/ 238 U vs. 232 Th/ 238 U) are also shown.

Appendix Figure 1: Photograph of the Alfalfa Site (El Paso, TX) and soil sample photos under microscope. Alfalfa soils consist of fine sands, silts, and clays, with roots and large soil aggregates. Pedogenic carbonates mainly occur as fine nodules, films, and filaments in soil matrix.

Appendix Figure 2: Photograph of the JPT1 Site in Jornada Range in New Mexico and soil and caliche sample photos under microscope. A caliche layer was observed at ~40 cm depth at the bottom of the soil pit. The selected caliche samples (~4 cm by 6 cm size) and the scrapped locations on the caliche are shown. Jornada soils consist of fine sands, silts, and clays, with roots and large gravels. Pedogenic carbonates mainly occur as both fine nodules, films, and filaments in soil matrix and thick coatings on gravels.

Appendix Figure 3: Photograph of the JPT2 Site in Jornada Range in New Mexico and soil and caliche sample photos under microscope. A caliche layer was observed at ~48 cm depth at the bottom of the soil pit. The selected caliche samples (~3 cm by 5 cm size) and the scrapped locations on the caliche are shown. Jornada soils consist of fine sands, silts, and clays, with roots and large gravels. Pedogenic carbonates mainly occur as both fine nodules, films, and filaments in soil matrix and thick coatings on gravels.

Appendix Figure 4: U-series isochron plots (²³⁰Th/²³⁸U vs. ²³²Th/²³⁸U and ²³⁴U/²³⁸U vs. ²³²Th/²³⁸U) for bulk soil and caliche samples in Alfalfa and Jornada profiles.

Table 1: Mineralogy, carbon contents, major element, Useries isotope concentrations and activity ratios, and

calculated U-series isotopes ages for pedogenic carbonates in Alfalfa and Jornada (JPT1 and JPT2) samples.

Depth	calcite to	SC	SOC	SIC b	CaO	Uc	Th	(²³⁴ U/ ²³⁸ U) bulk soil	(²³⁰ Th/ ²³⁸ U) bulk soil	Carbonate Age U dating
(cm)	quartz ^a	wt%	wt%	b wt% wt% ppm		ppm	ppm			(Ka)
							C			
1.5	0.23	1.67	0.82	0.85	4.83	2.31	8.09	1.01	1.21	15±17
11.5	0.16	1.48	0.57	0.91	4.93	2.53	9.58	1.00	1.03	6.5±8.7
21.5	0.33	1.38	0.49	0.89	4.79	2.33	7.66	1.01	1.08	9.1±8.6
31.5	0.18	1.33	0.50	0.83	4.69	2.45	8.07	1.00	1.04	5.1 ± 5.7
41.5	0.22	1.31	0.39	0.93	5.35	2.46	7.73	1.00	1.08	2.2 ± 1.7
51.5	0.16	0.94	0.18	0.76	4.45	2.12	6.58	0.98	0.75	2.9±1.9
61.5	0.10	0.57	0.07	0.50	2.87	1.94	6.24	0.97	1.00	22.2±8.1
	(cm) 1.5 11.5 21.5 31.5 41.5 51.5	to quartza (cm) 1.5 0.23 11.5 0.16 21.5 0.33 31.5 0.18 41.5 0.22 51.5 0.16	to quartza SC (cm) wt% 1.5 0.23 1.67 11.5 0.16 1.48 21.5 0.33 1.38 31.5 0.18 1.33 41.5 0.22 1.31 51.5 0.16 0.94	to quartza SC SOC (cm) wt% wt% 1.5 0.23 1.67 0.82 11.5 0.16 1.48 0.57 21.5 0.33 1.38 0.49 31.5 0.18 1.33 0.50 41.5 0.22 1.31 0.39 51.5 0.16 0.94 0.18	to quartza SC SOC SIC b (cm) wt% wt% wt% 1.5 0.23 1.67 0.82 0.85 11.5 0.16 1.48 0.57 0.91 21.5 0.33 1.38 0.49 0.89 31.5 0.18 1.33 0.50 0.83 41.5 0.22 1.31 0.39 0.93 51.5 0.16 0.94 0.18 0.76	to quartza SC SOC SIC b CaO (cm) wt% wt% wt% wt% 1.5 0.23 1.67 0.82 0.85 4.83 11.5 0.16 1.48 0.57 0.91 4.93 21.5 0.33 1.38 0.49 0.89 4.79 31.5 0.18 1.33 0.50 0.83 4.69 41.5 0.22 1.31 0.39 0.93 5.35 51.5 0.16 0.94 0.18 0.76 4.45	to quartza SC SOC SIC b CaO Uc (cm) wt% wt% wt% wt% ppm 1.5 0.23 1.67 0.82 0.85 4.83 2.31 11.5 0.16 1.48 0.57 0.91 4.93 2.53 21.5 0.33 1.38 0.49 0.89 4.79 2.33 31.5 0.18 1.33 0.50 0.83 4.69 2.45 41.5 0.22 1.31 0.39 0.93 5.35 2.46 51.5 0.16 0.94 0.18 0.76 4.45 2.12	Depth to quartza SC SOC SIC b CaO Uc Th (cm) wt% wt% wt% wt% ppm ppm 1.5 0.23 1.67 0.82 0.85 4.83 2.31 8.09 11.5 0.16 1.48 0.57 0.91 4.93 2.53 9.58 21.5 0.33 1.38 0.49 0.89 4.79 2.33 7.66 31.5 0.18 1.33 0.50 0.83 4.69 2.45 8.07 41.5 0.22 1.31 0.39 0.93 5.35 2.46 7.73 51.5 0.16 0.94 0.18 0.76 4.45 2.12 6.58	Depth to quartza SC soc soc sic soc soc sic soc soc soc soc soc soc soc soc soc so	to quartza SC SOC SIC b b CaO U° Th bulk soil bulk soil bulk soil (cm) wt% wt% wt% wt% ppm ppm ppm 1.5 0.23 1.67 0.82 0.85 4.83 2.31 8.09 1.01 1.21 11.5 0.16 1.48 0.57 0.91 4.93 2.53 9.58 1.00 1.03 21.5 0.33 1.38 0.49 0.89 4.79 2.33 7.66 1.01 1.08 31.5 0.18 1.33 0.50 0.83 4.69 2.45 8.07 1.00 1.04 41.5 0.22 1.31 0.39 0.93 5.35 2.46 7.73 1.00 1.08 51.5 0.16 0.94 0.18 0.76 4.45 2.12 6.58 0.98 0.75

Average carbonate age for the entire profile: 7.3 ± 5.0 Ka; accumulation rate of CaCO₃ (g m⁻² yr⁻¹): 9 ± 6

JPT1											
0-10cm	5.0	0.36	2.96	0.42	2.54	12.8	1.94	8.91	0.95	1.23	44±32
10-15cm	12.5	0.40	3.52	0.52	2.99	13.9	2.04	6.41	0.97	1.21	17.1±6
15-20cm	17.5	0.85	4.94	0.48	4.45	20.3	1.89	6.17	1.00	1.20	30±11
25-30cm	27.5	0.81	4.37	0.49	3.88	20.1	1.95	6.40	1.00	1.19	14.5±6.8
40cm	40.0	3.99	9.11	0.38	8.73	45.6	1.14	2.35	1.18	0.92	117±26

Average carbonate age for the entire profile: 28 ± 11 Ka; accumulation rate of CaCO₃ (g m⁻² yr⁻¹): 3.5 ± 1.5

JPT2											
0-7cm	3.5	0.35	1.51	0.41	1.10	9.92	1.95	8.72	0.96	1.54	68±110
7-10cm	8.5	0.39	2.60	0.57	2.03	15.7	1.76	6.32	0.97	1.18	29±13
27-30cm	28.5	0.52	2.43	0.59	1.84	13.8	1.95	6.10	0.99	1.18	19.5±7.5
37-40cm	38.5	0.44	2.64	0.78	1.86	14.7	1.84	7.00	0.99	1.18	50±21
48cm	48.0	2.72	5.82	0.43	5.39	46.2	1.30	1.56	1.30	0.75	100±40

Average carbonate age for the entire profile: 34 ± 14 Ka; accumulation rate of CaCO₃ (g m⁻² yr⁻¹): 2.5 ± 1.0

a: XRD intensity peak ratio of calcite to quartz

b: calculated SIC = SC - SOC

c: uncertainty for U and Th concentrations and (234U/238U) and (230Th/238U) is 1%;

d: see appendix Table and Figures for detailed U-series age calculation in pedogenic carbonates

Table 2: The U-Th activity rations for bulk soil and caliche samples, acid leachate and residual, water leachate and residual samples for Alfalfa and Jornada profiles. Correlation coefficients (R^2) for isochron plots (230 Th/ 238 U vs. 232 Th/ 238 U and 234 U/ 238 U vs. 232 Th/ 238 U) are also shown. Graphs are in Appendix Figures.

Sample Name	Туре	(²³⁴ U/ ²³⁸ U)	+/-	(²³⁰ Th/ ²³⁸ U)	+/-	(²³² Th/ ²³⁸ U)	+/-	R ² (1)*	R ² (2)*
Alfalfa	Bulk soil	1.009	0.005	1.211	0.012	1.145	0.011	0.88	0.95
0-3cm	HCI L	1.290	0.006	0.652	0.007	0.464	0.005		
	HCI R	0.969	0.005	1.306	0.013	1.227	0.012		
	H₂O S	1.037	0.005	1.542	0.015	1.224	0.012		
	H₂O R	1.003	0.005	1.154	0.012	1.117	0.011		
Alfalfa	Bulk soil	1.001	0.005	1.034	0.010	1.240	0.012	0.95	0.90
10-13cm	HCI L	1.346	0.007	0.461	0.005	0.436	0.004		
	HCI R	0.957	0.005	1.151	0.012	1.222	0.012		
	H ₂ O S	1.021	0.005	1.281	0.013	1.306	0.013		
	H₂O R	1.000	0.005	1.020	0.010	1.054	0.011		
Alfalfa	Bulk soil	1.011	0.005	1.079	0.011	1.074	0.011	0.95	0.86
20-23cm	HCI L	1.300	0.006	0.689	0.007	0.620	0.006		
	HCI R	0.974	0.005	1.162	0.012	1.169	0.012		
	H₂O S	1.039	0.005	1.309	0.013	1.269	0.013		
	H₂O R	1.003	0.005	1.053	0.011	1.142	0.011		
Alfalfa	Bulk soil	1.001	0.005	1.083	0.017	1.078	0.013	0.99	0.52
30-33cm	HCI L	1.308	0.007	0.639	0.010	0.575	0.007		
	HCI R	0.964	0.701	1.344	0.021	1.333	0.016		
	H₂O S	1.031	0.224	1.970	0.032	1.931	0.023		
	H ₂ O R	0.991	0.882	1.498	0.024	1.569	0.019		
Alfalfa	Bulk soil	1.003	0.005	1.045	0.010	1.028	0.010	0.99	0.93
40-43cm	HCI L	1.440	0.007	0.111	0.001	0.085	0.001		
	HCI R	0.950	0.005	1.163	0.012	1.194	0.012		

	H₂O S	1.060	0.005	1.185	0.012	1.167	0.012		
	H₂O R	0.991	0.005	1.008	0.010	1.017	0.010		
Alfalfa	Bulk soil	0.989	0.005	0.747	0.012	1.018	0.012	0.99	0.66
50-53cm	HCI L	1.223	0.006	0.293	0.005	0.369	0.004		
	HCI R	0.954	0.005	0.927	0.015	1.312	0.016		
	H ₂ O S	1.042	0.005	1.135	0.018	1.548	0.019		
	H₂O R	0.977	0.005	1.074	0.017	1.501	0.018		
Alfalfa	Bulk soil	0.968	0.005	1.001	0.016	1.055	0.013	0.98	0.19
60-63cm	HCI L	1.125	0.006	0.869	0.014	0.866	0.010		
	HCI R	0.950	0.005	1.043	0.017	1.097	0.013		
	H₂O S	1.027	0.005	1.203	0.019	1.324	0.016		
	H₂O R	0.968	0.005	0.989	0.016	1.084	0.013		
JPT1	Bulk soil	0.954	0.005	1.233	0.020	1.503	0.018	0.71	0.85
0-10cm	HCI L	1.152	0.006	0.909	0.015	0.757	0.009		
	HCI R	0.940	0.005	1.356	0.022	1.366	0.016		
	H ₂ O S	0.965	0.005	1.511	0.024	1.416	0.017		
	H ₂ O R	0.965	0.005	1.182	0.019	1.179	0.014		
JPT1	Bulk soil	0.967	0.005	1.208	0.019	1.029	0.012	0.99	0.01
10-15cm	HCI L	1.159	0.006	1.071	0.017	0.918	0.011		
	HCI R	0.988	0.005	1.308	0.021	1.199	0.014		
	H ₂ O S	0.976	0.005	0.378	0.006	0.346	0.004		
	H ₂ O R	1.001	0.005	4.729	0.076	4.794	0.058		
JPT1	Bulk soil	1.004	0.005	1.204	0.019	1.068	0.013	0.94	0.91
15-20cm	HCI L	1.226	0.006	0.852	0.014	0.594	0.007		
	HCI R	0.965	0.005	1.309	0.021	1.170	0.014		
	H₂O S	1.034	0.005	1.385	0.022	1.176	0.014		
	H₂O R	0.995	0.005	1.176	0.019	1.092	0.013		

JPT1	Bulk soil	1.003	0.005	1.192	0.019	1.076	0.013	0.98	0.87
25-30cm	HCI L	1.233	0.006	0.643	0.010	0.476	0.006		
	HCI R	0.977	0.005	1.244	0.020	1.116	0.013		
	H ₂ O S	1.042	0.005	1.361	0.022	1.176	0.014		
	H₂O R	0.988	0.005	1.128	0.018	1.051	0.013		
JPT2	Bulk soil	0.962	0.005	1.535	0.025	1.463	0.018	0.07	0.46
0-7cm	HCI L	1.216	0.006	1.289	0.021	1.173	0.014		
	HCI R	0.967	0.005	1.167	0.019	1.517	0.018		
	H ₂ O S	0.963	0.005	1.614	0.026	1.395	0.017		
	H₂O R	0.954	0.005	1.169	0.019	1.242	0.015		
JPT2	Bulk soil	0.970	0.005	1.185	0.019	1.173	0.014	0.91	0.88
7-10cm	HCI L	1.223	0.006	0.828	0.013	0.610	0.007		
	HCI R	0.943	0.005	1.237	0.020	1.222	0.015		
	H ₂ O S	0.993	0.005	1.399	0.022	1.255	0.015		
	H ₂ O R	0.960	0.005	1.111	0.018	1.071	0.013		
JPT2	Bulk soil	0.994	0.005	1.183	0.019	1.022	0.012	0.93	0.85
27-30cm	HCI L	1.207	0.006	0.802	0.013	0.601	0.007		
	HCI R	0.969	0.005	1.248	0.020	1.130	0.014		
	H ₂ O S	1.023	0.005	1.347	0.022	1.132	0.014		
	H ₂ O R	0.988	0.005	1.138	0.018	0.978	0.012		
JPT2	Bulk soil	0.994	0.005	1.176	0.019	1.246	0.015	0.72	0.85
37-40cm	HCI L	1.207	0.006	0.990	0.016	0.769	0.009		
	HCI R	0.969	0.005	1.202	0.019	1.139	0.014		
	H ₂ O S	1.023	0.005	1.319	0.021	1.200	0.014		
	H₂O R	0.988	0.005	1.146	0.018	1.129	0.014		
JPT1	sub1	1.208	0.006	0.891	0.014	0.654	0.008	0.98	0.98
40cm	sub2	1.206	0.006	0.901	0.014	0.724	0.009		

Caliche	sub3	1.156	0.006	0.938	0.015	1.029	0.012		
	sub4	1.163	0.006	0.901	0.014	0.596	0.007		
	sub5	1.141	0.006	0.968	0.015	0.756	0.009		
JPT2	sub1	1.323	0.007	0.659	0.011	0.885	0.011	0.82	0.97
48cm	sub2	1.330	0.007	0.709	0.011	0.527	0.006		
Caliche	sub3	1.283	0.006	0.798	0.013	0.682	0.008		
	sub4	1.237	0.006	0.855	0.014	0.610	0.007		
	sub5	1.319	0.007	0.734	0.012	0.571	0.007		

^{*}Correlation coefficients (R^2) for isochron plots (230 Th/ 238 U vs. 232 Th/ 238 U) and (234 U/ 238 U vs. 232 Th/ 238 U) are reported as R^2 (1) and R^2 (2), respectively.



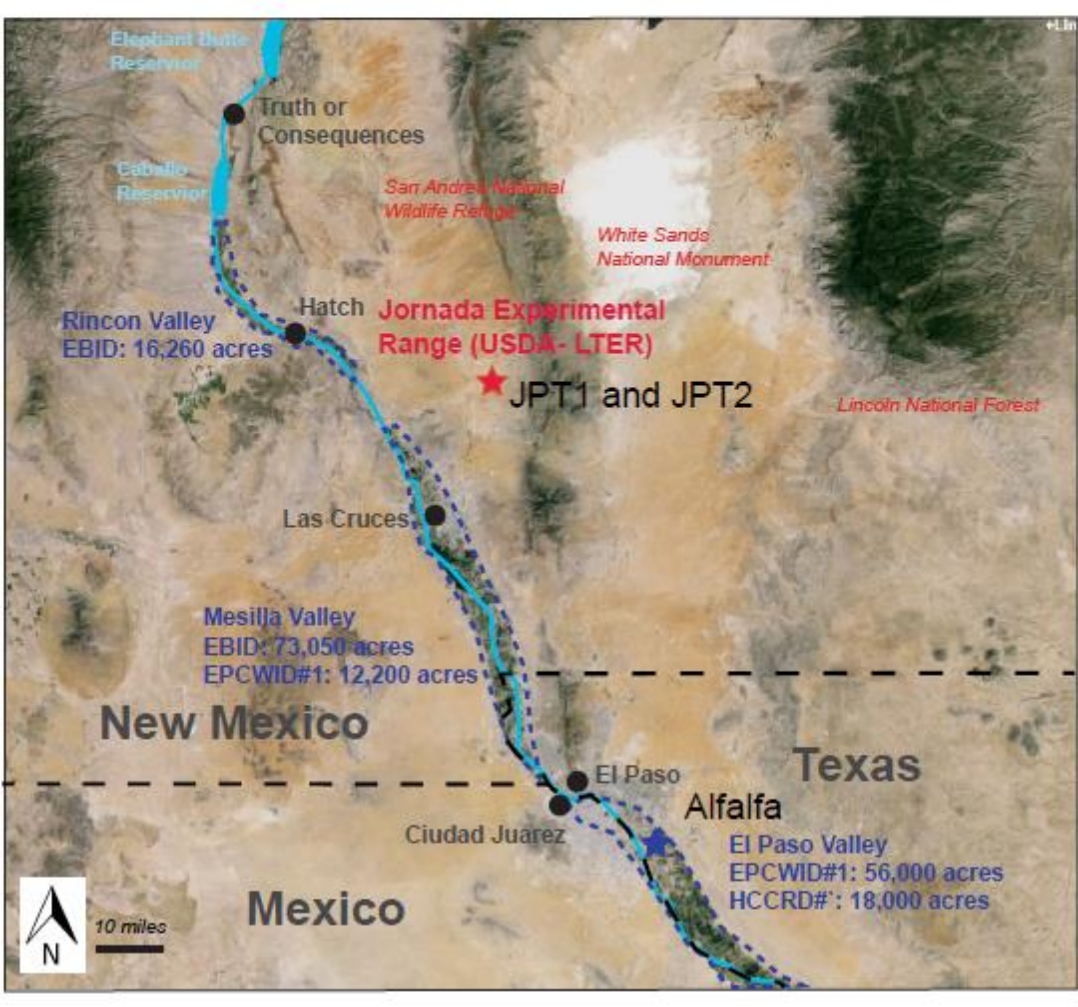


Figure 1

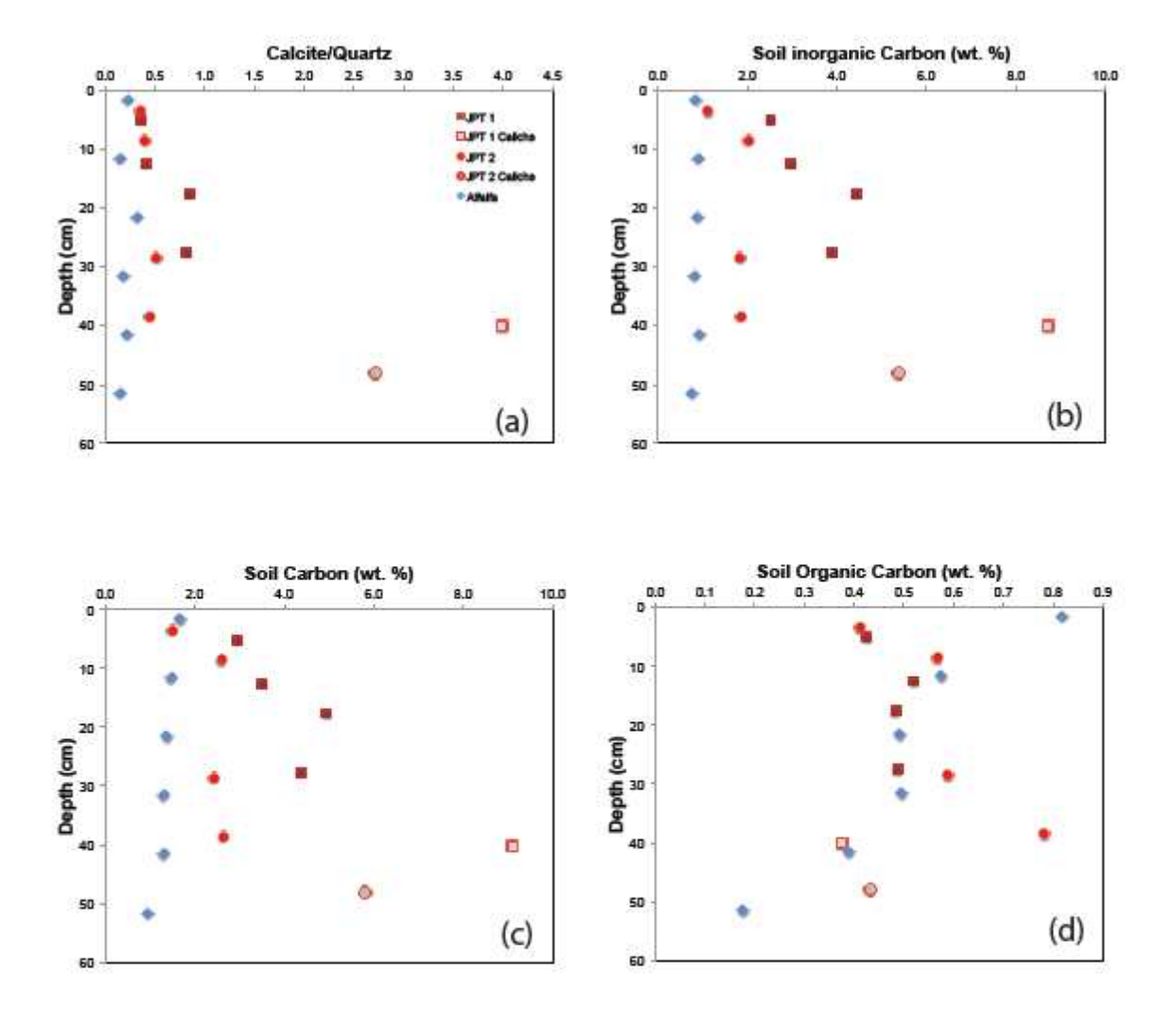
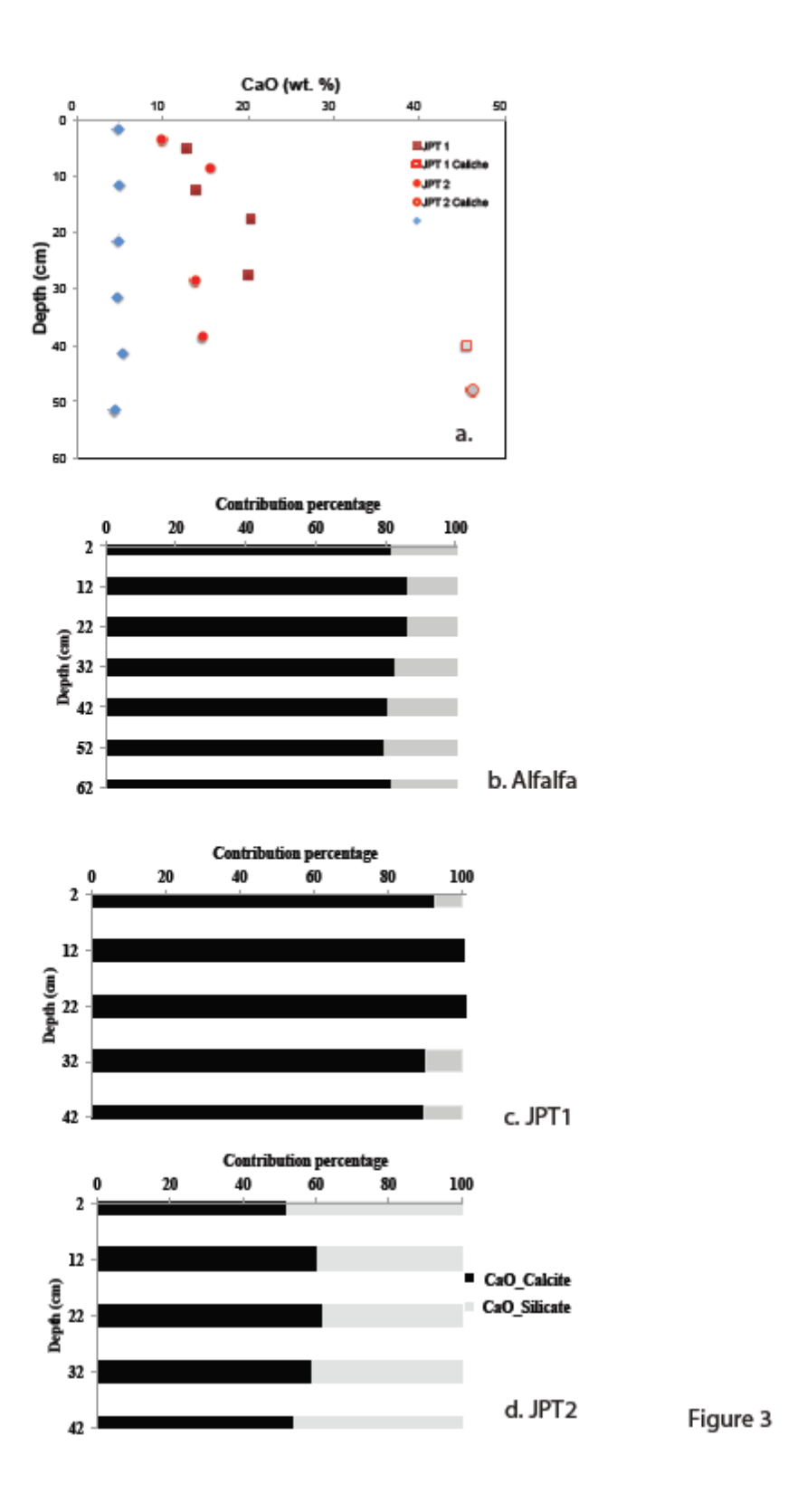
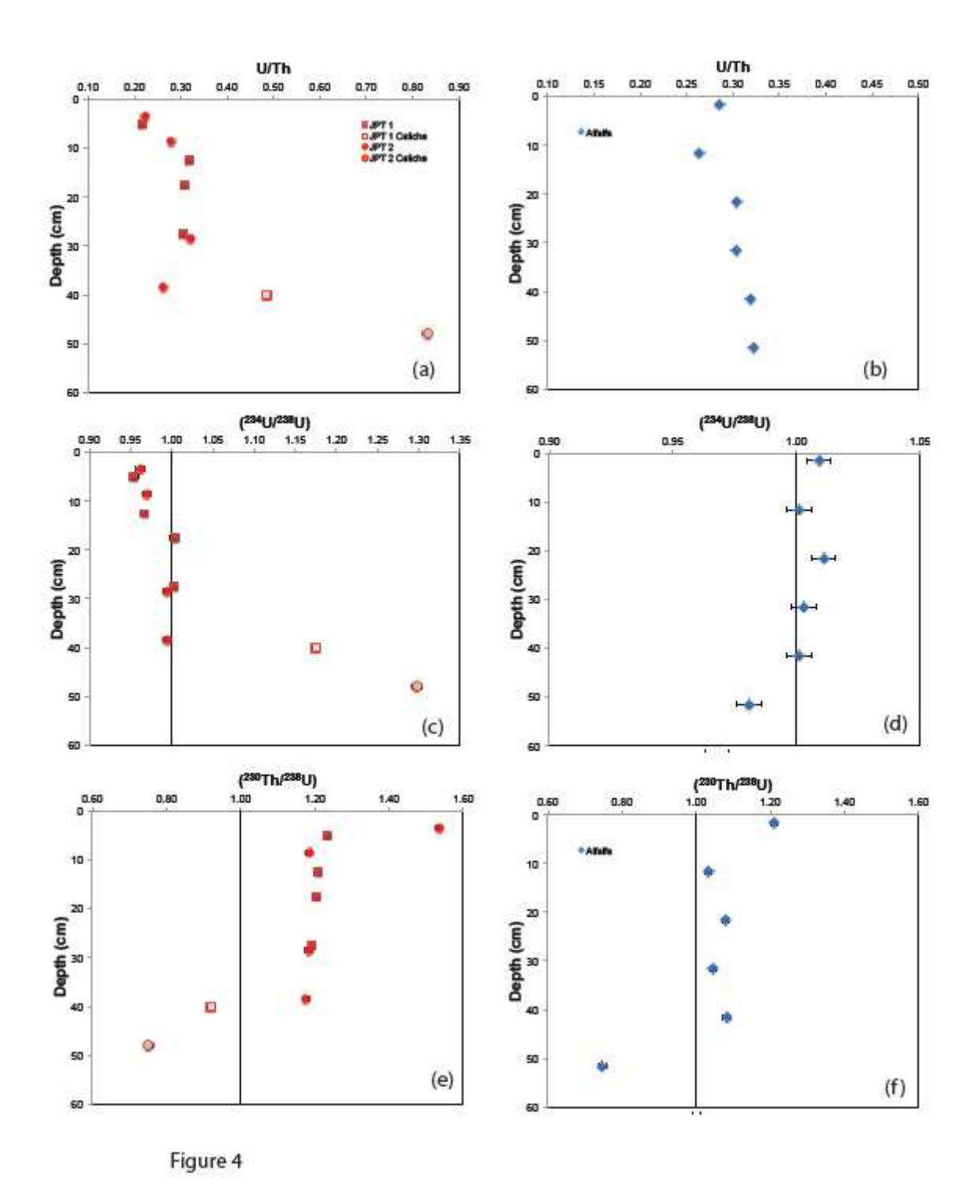


Figure 2





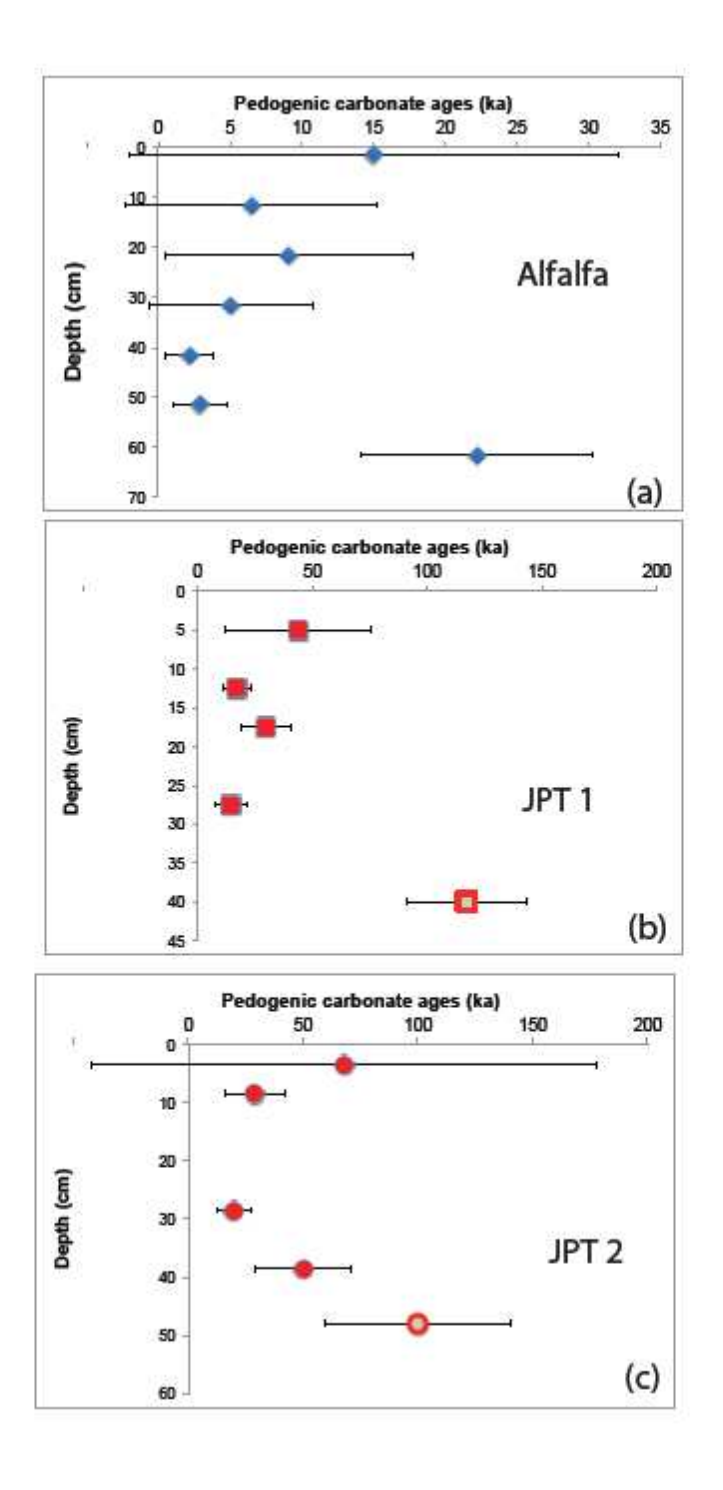
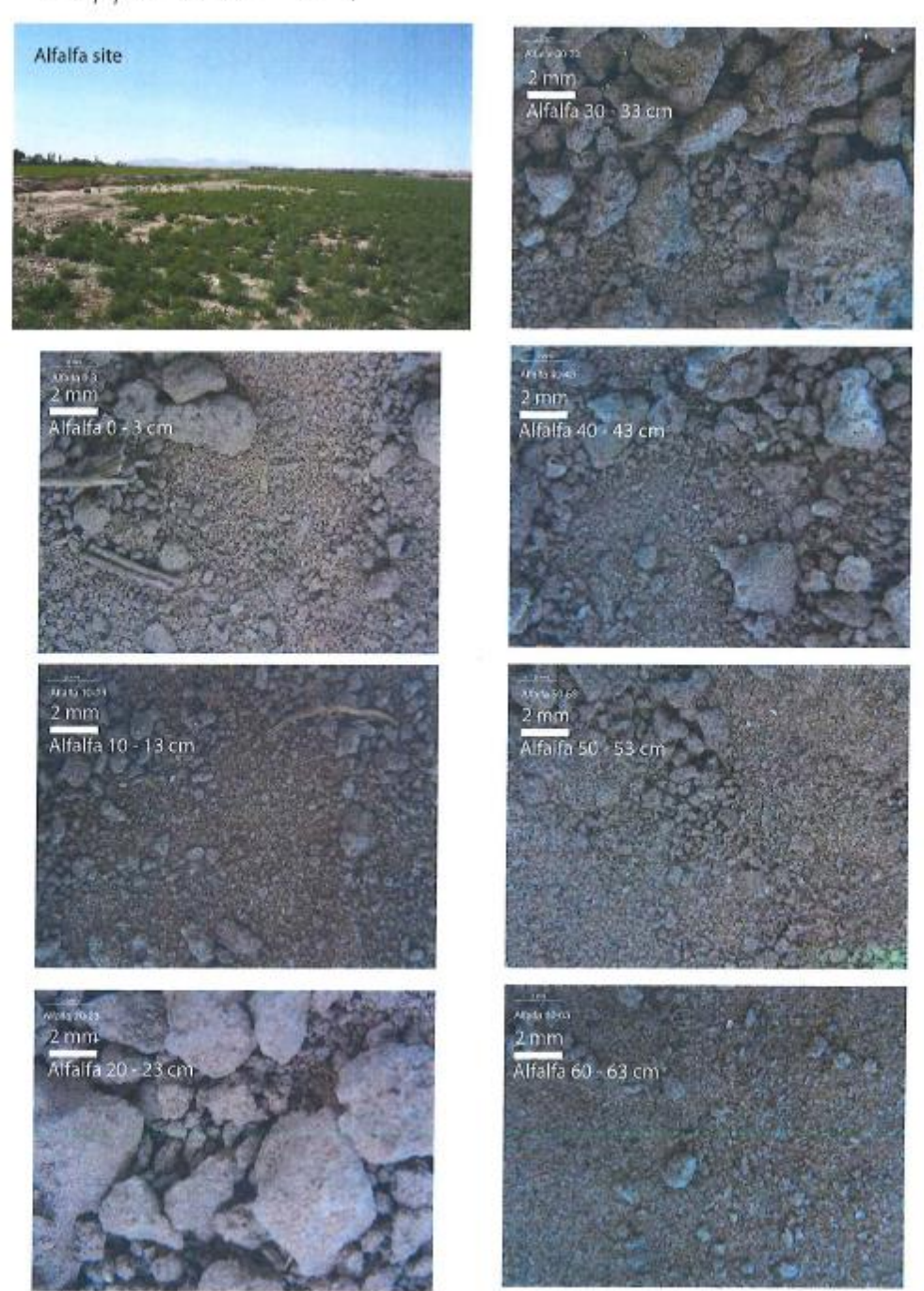
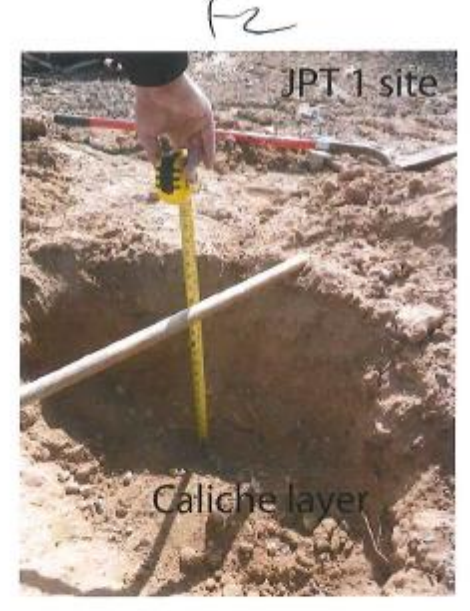


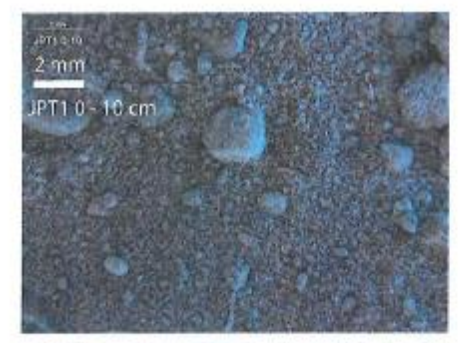
Figure 5

Appendix E1



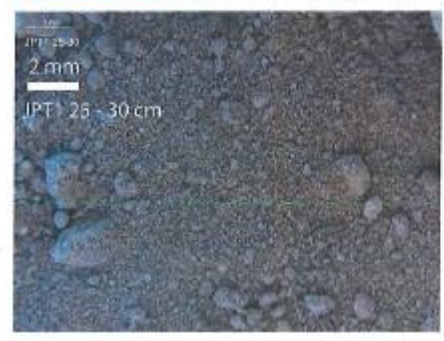




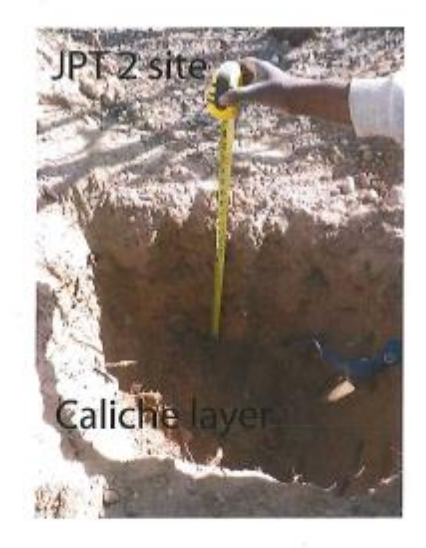




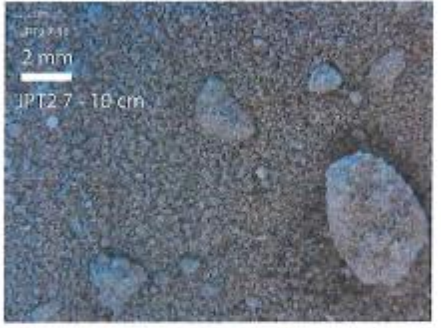






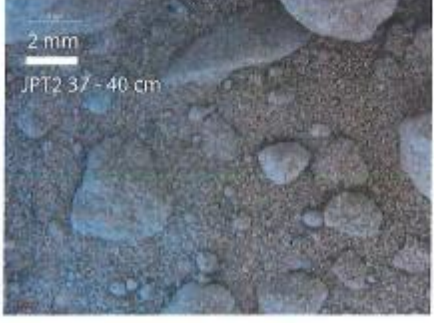


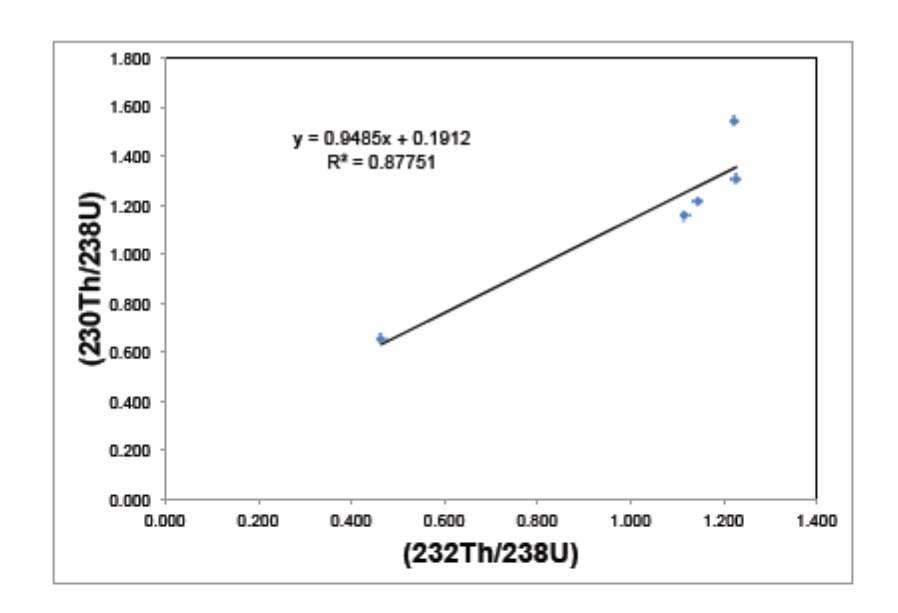


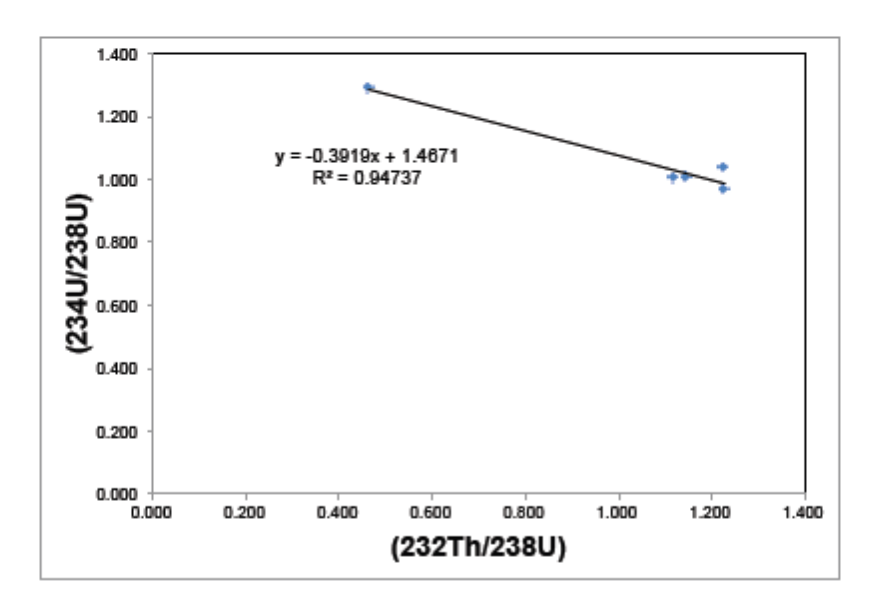




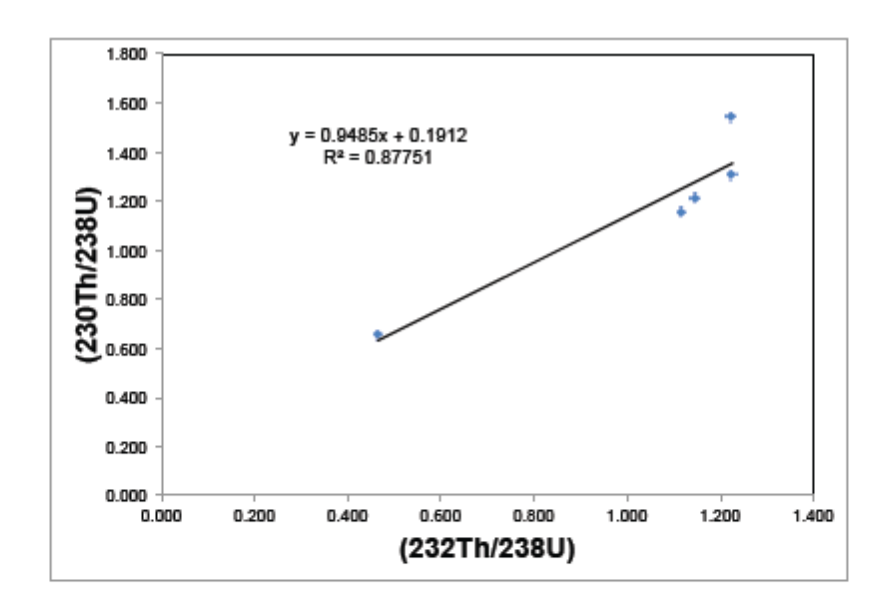


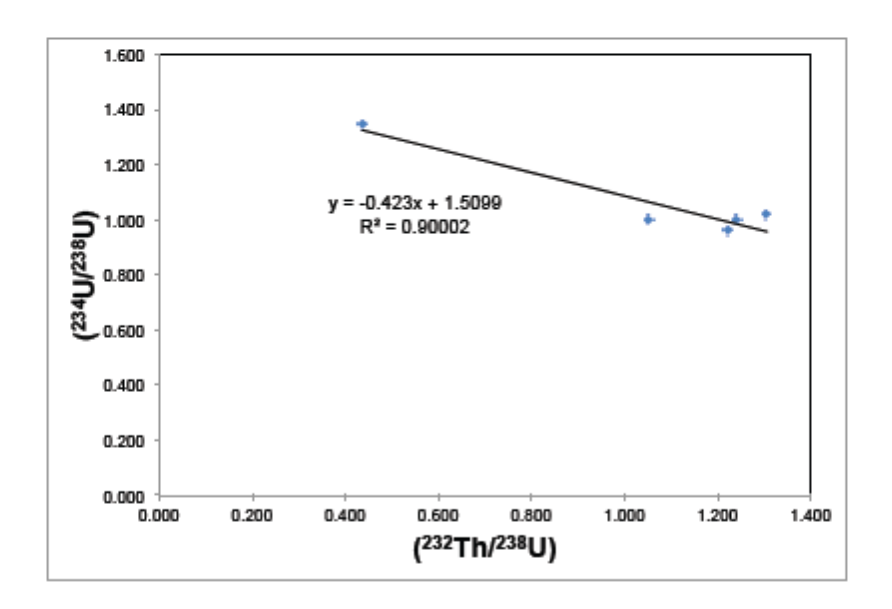




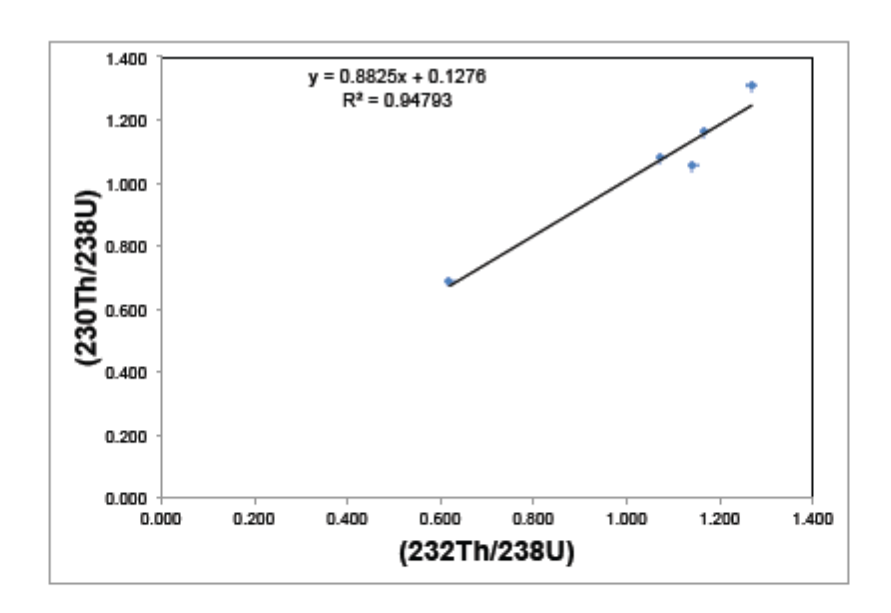


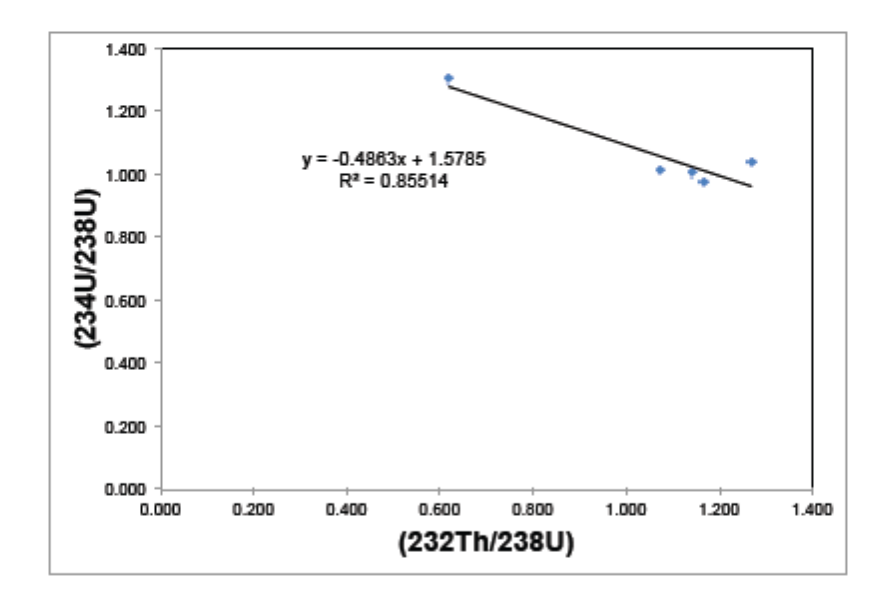
Alfalfa 0 to 3 cm



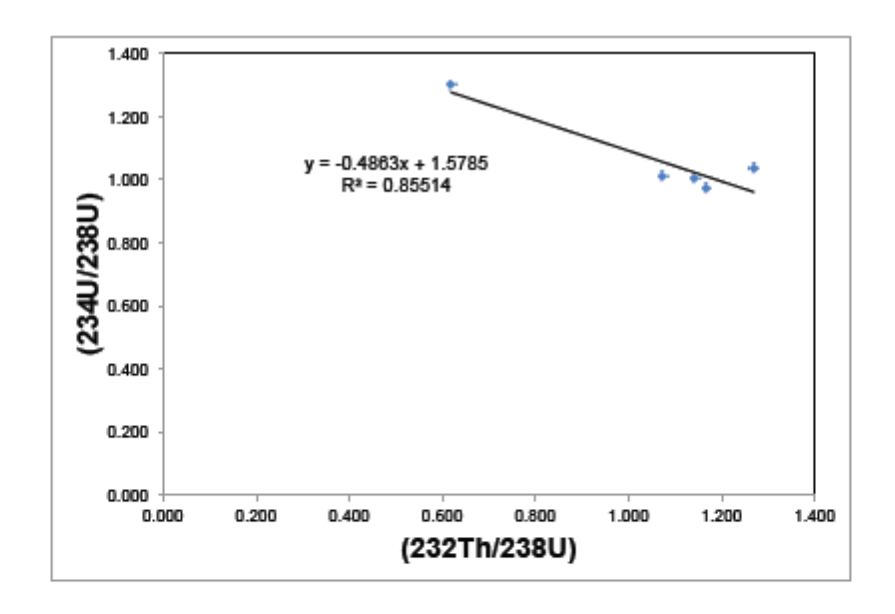


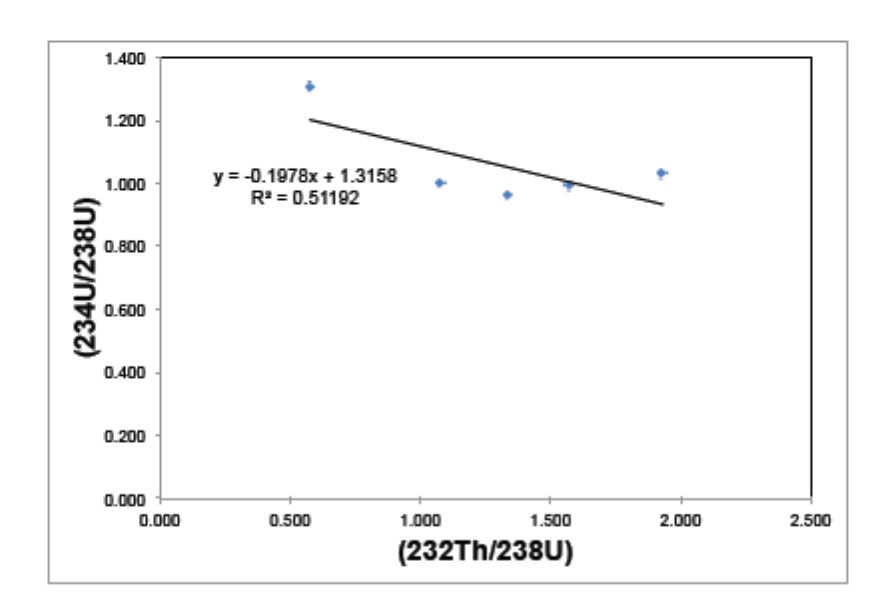
Alfalfa 10-13cm



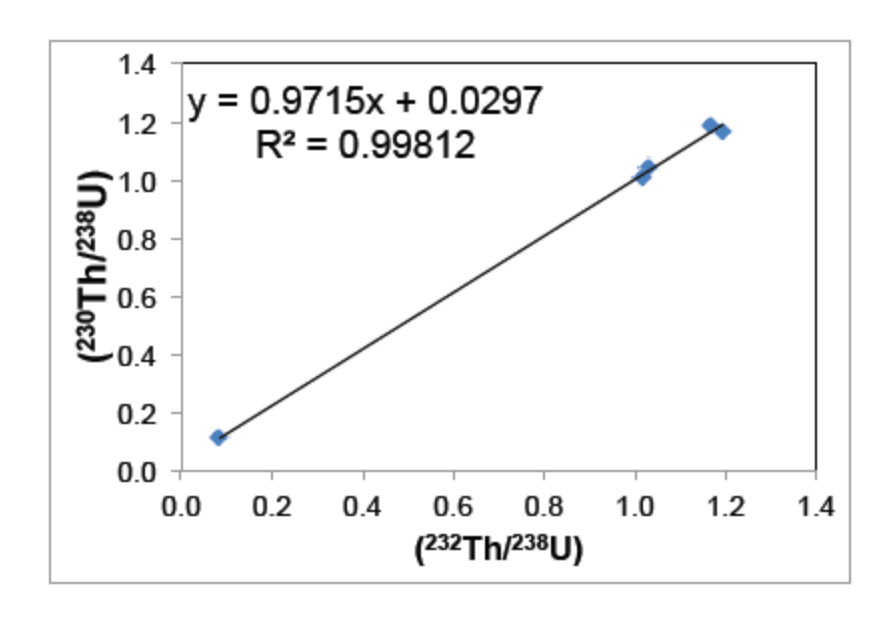


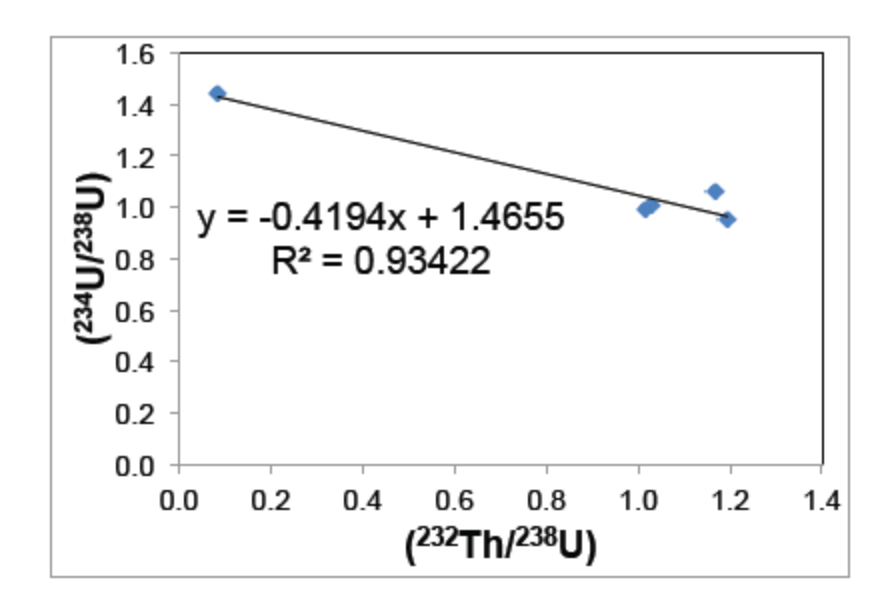
Alfalfa 20 to 23 cm



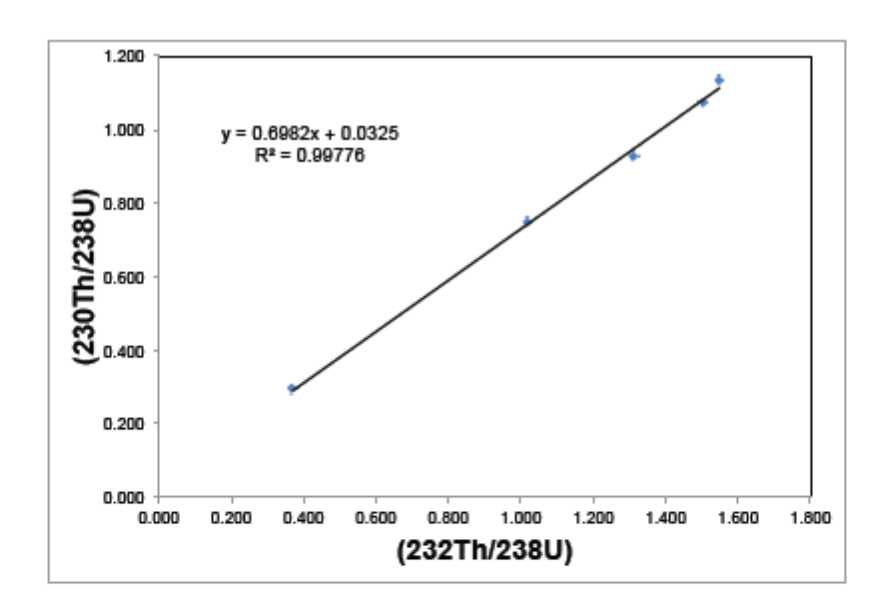


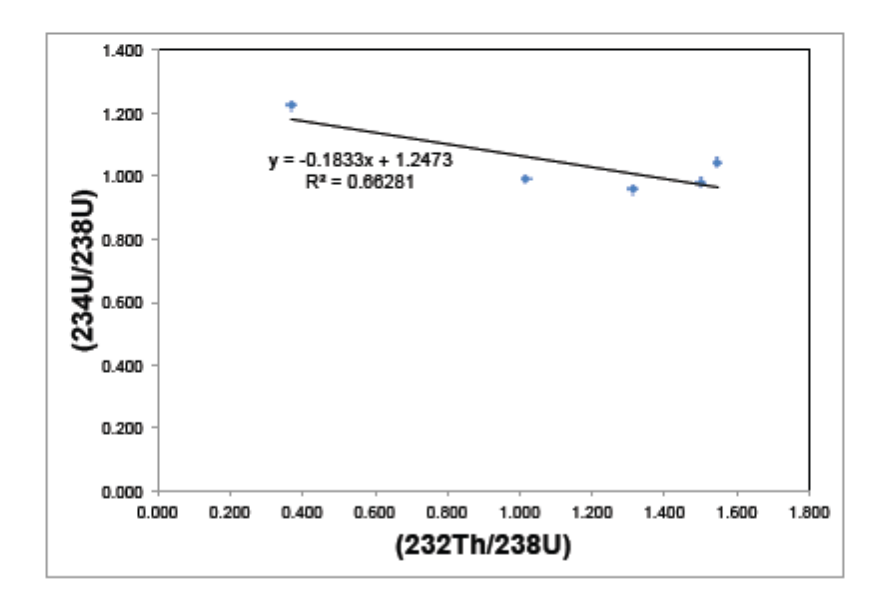
Alfalfa 30 to 33 cm



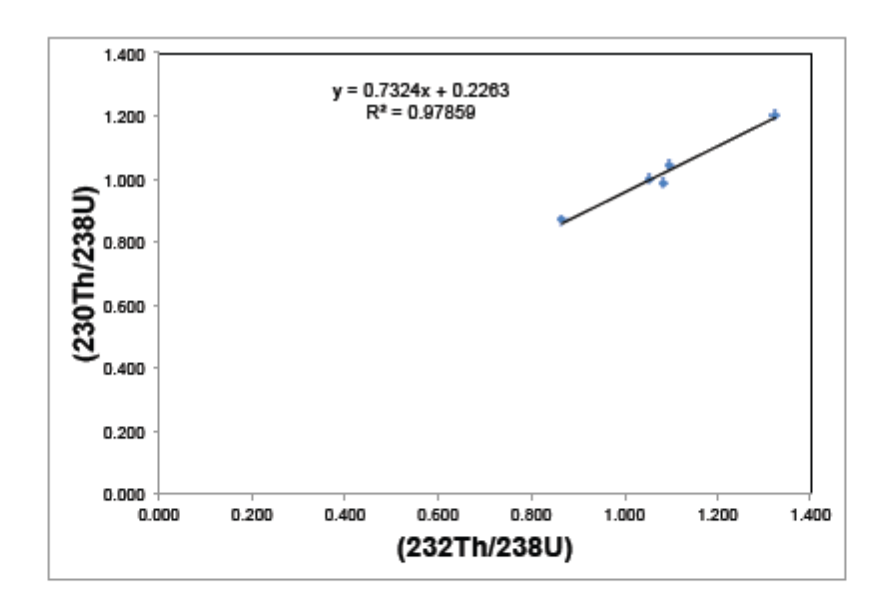


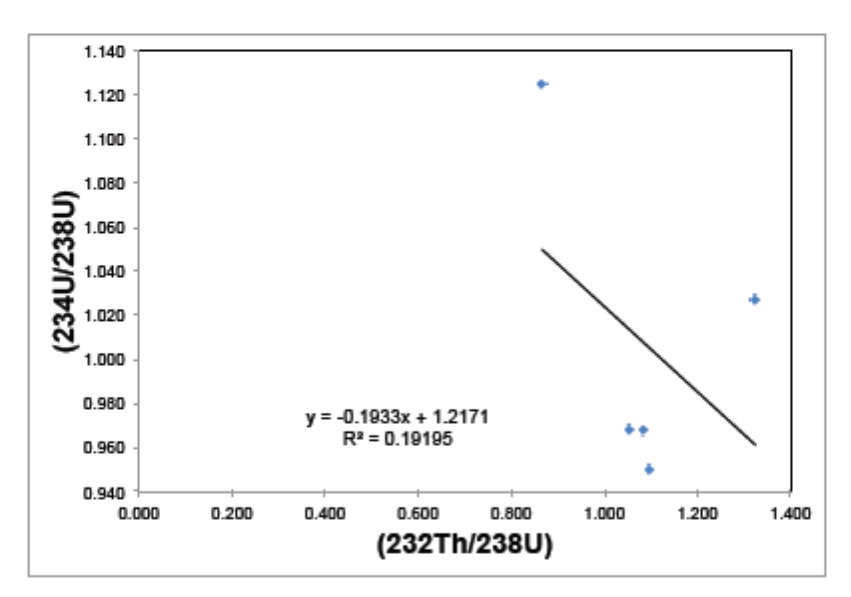
Alfalfa 40 to 43 cm



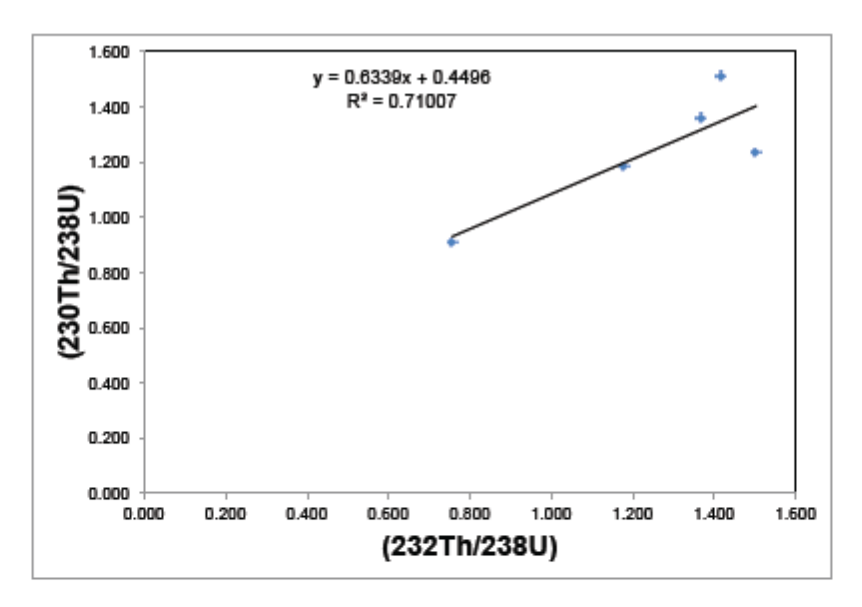


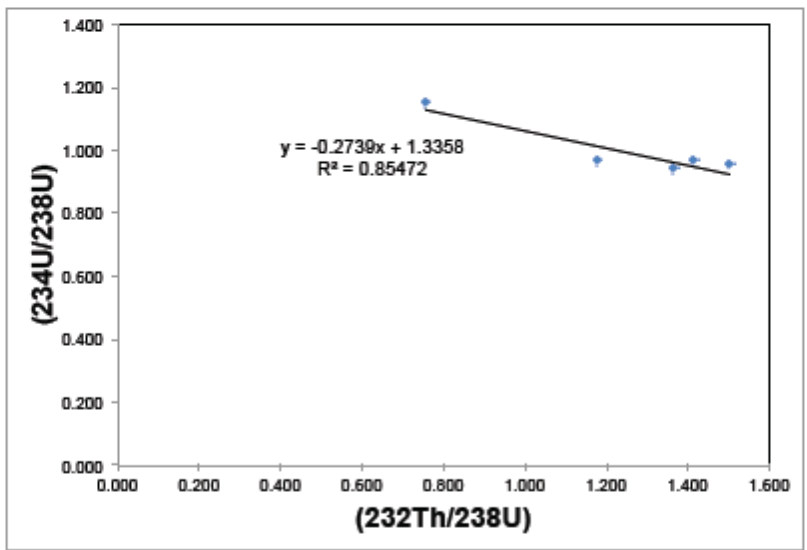
Alfalfa 50 to 53 cm



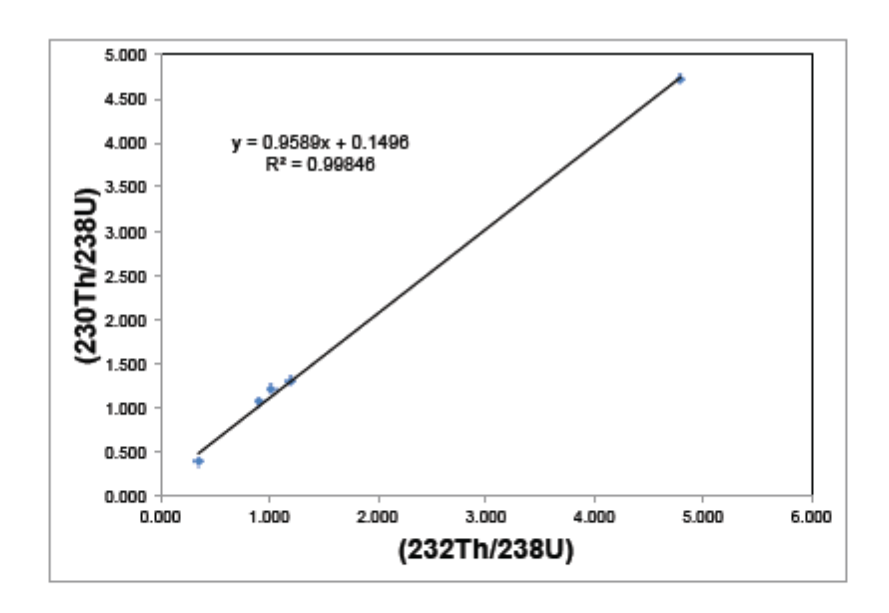


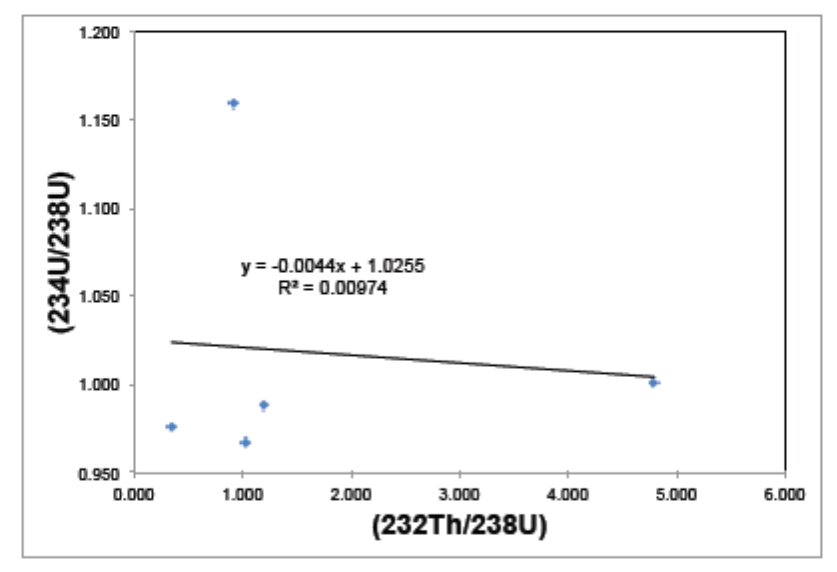
Alfalfa 60 to 63 cm



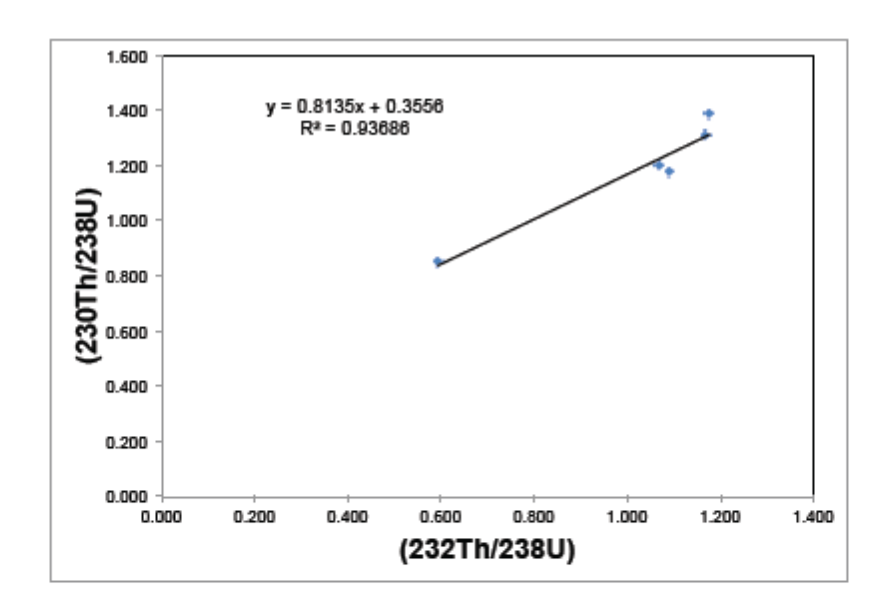


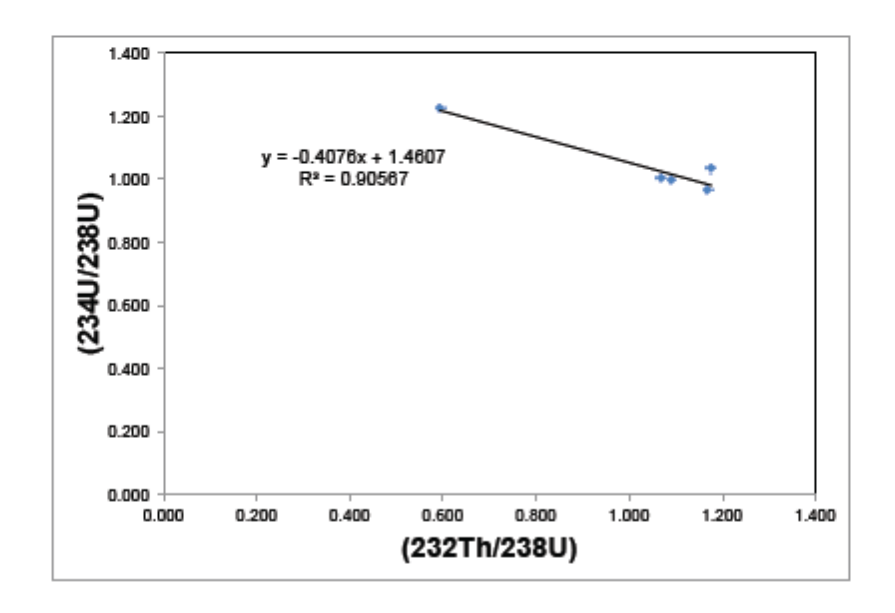
JPT1 0 to 10cm



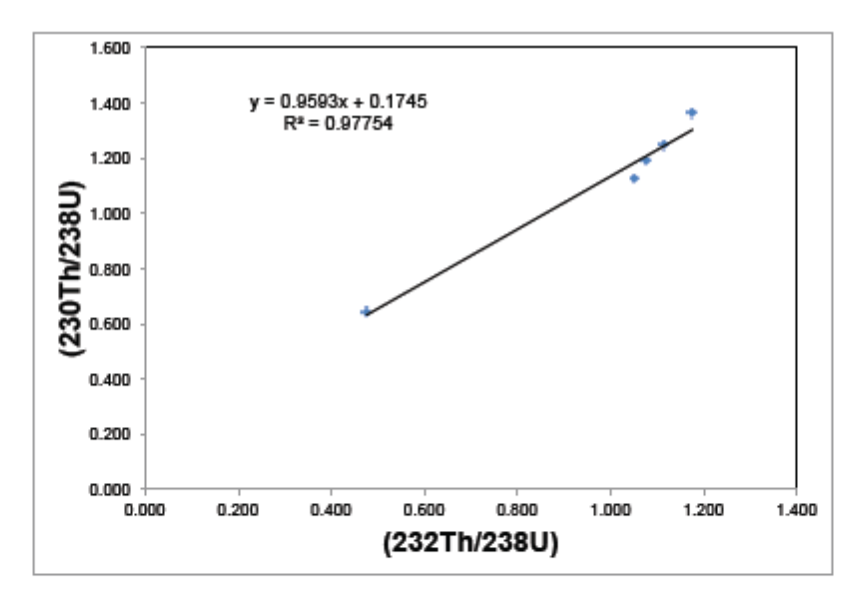


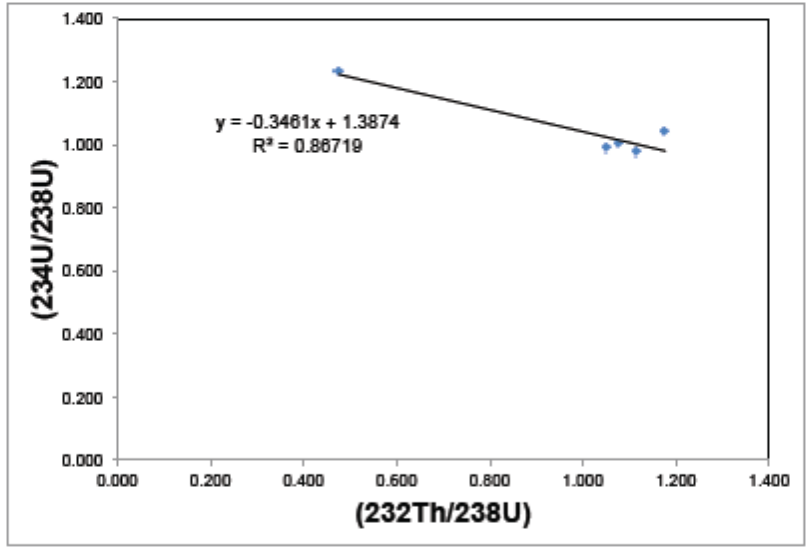
JPT1 10 to 15 cm



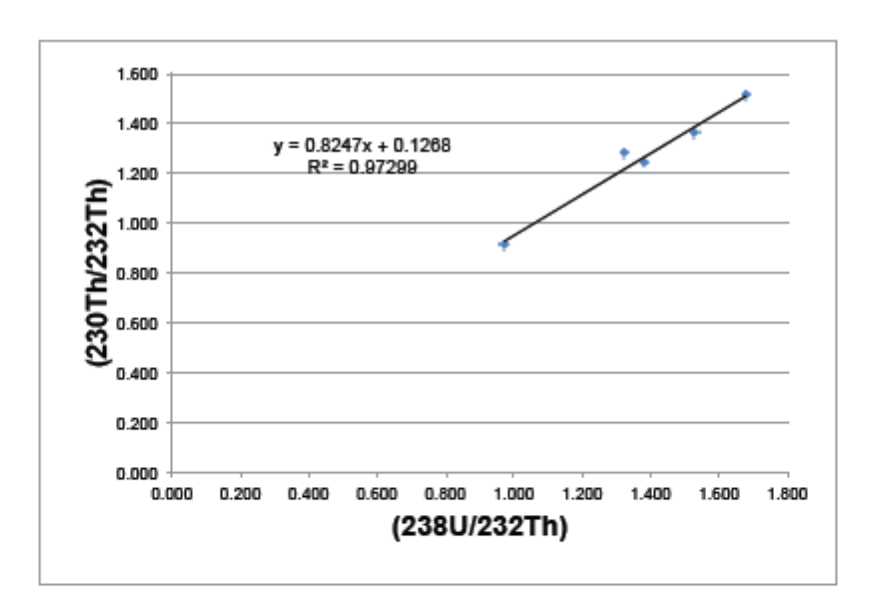


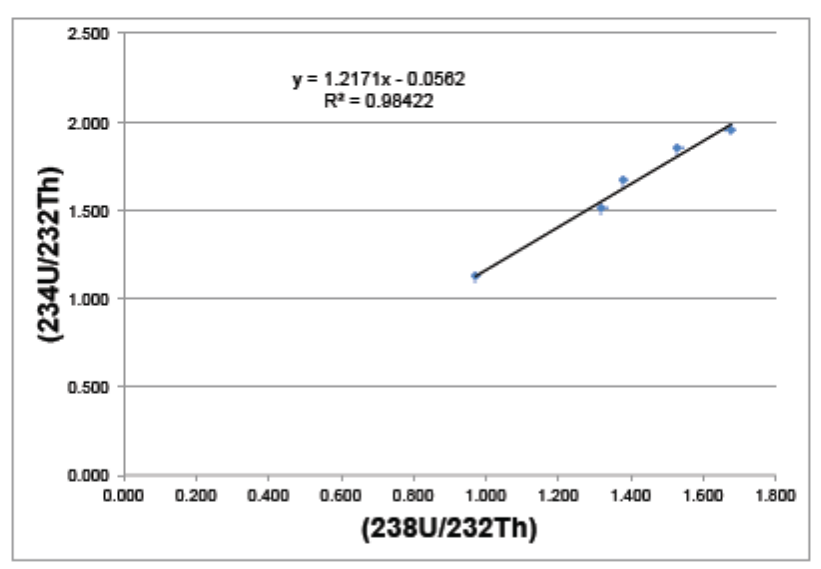
JPT1 15 to 20 cm



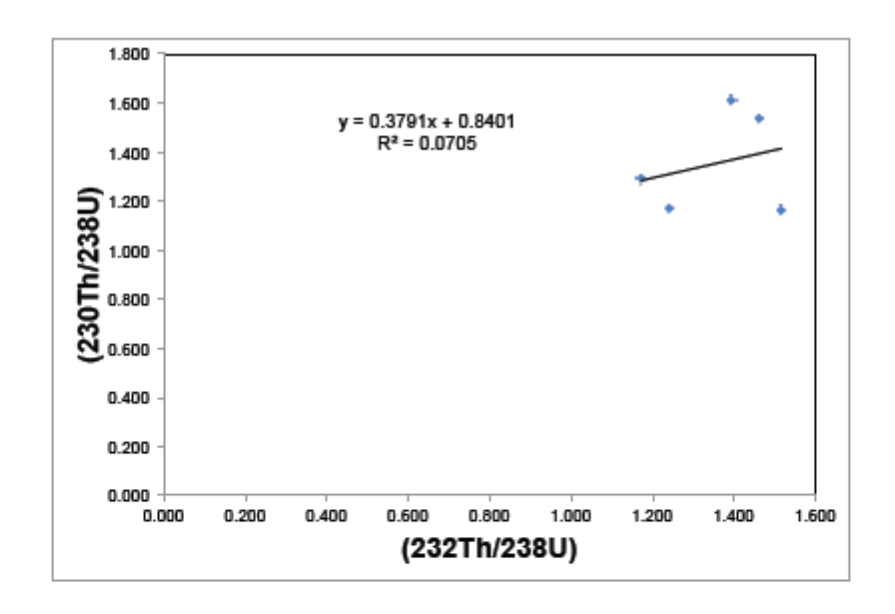


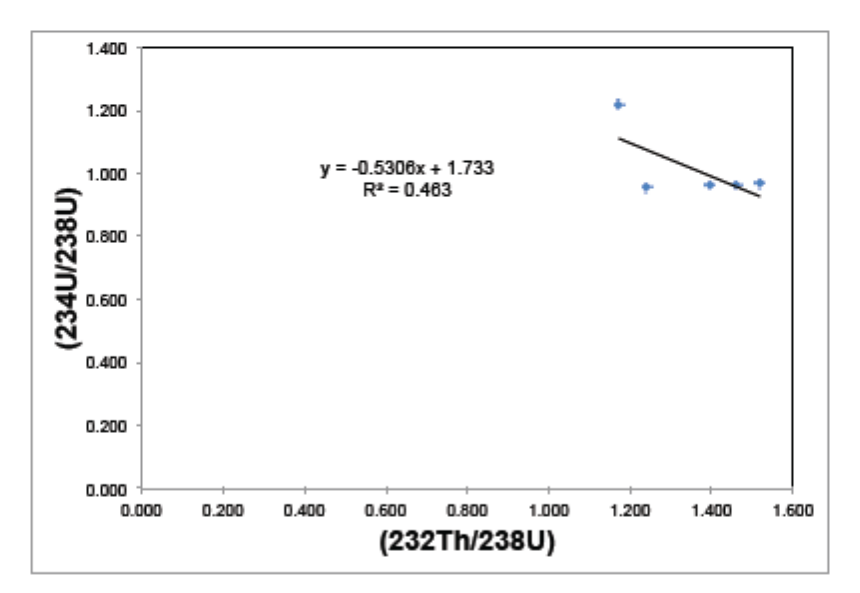
JPT1 25 to 30 cm



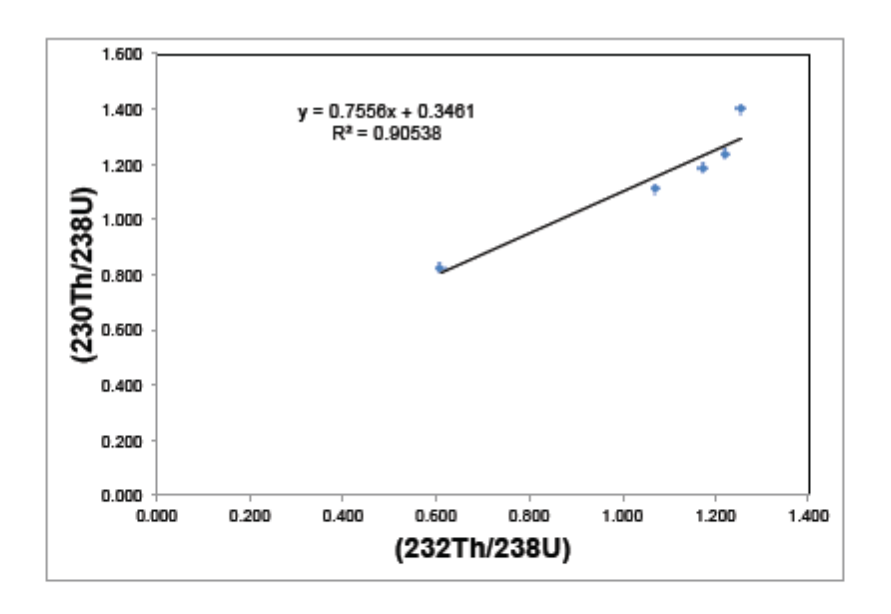


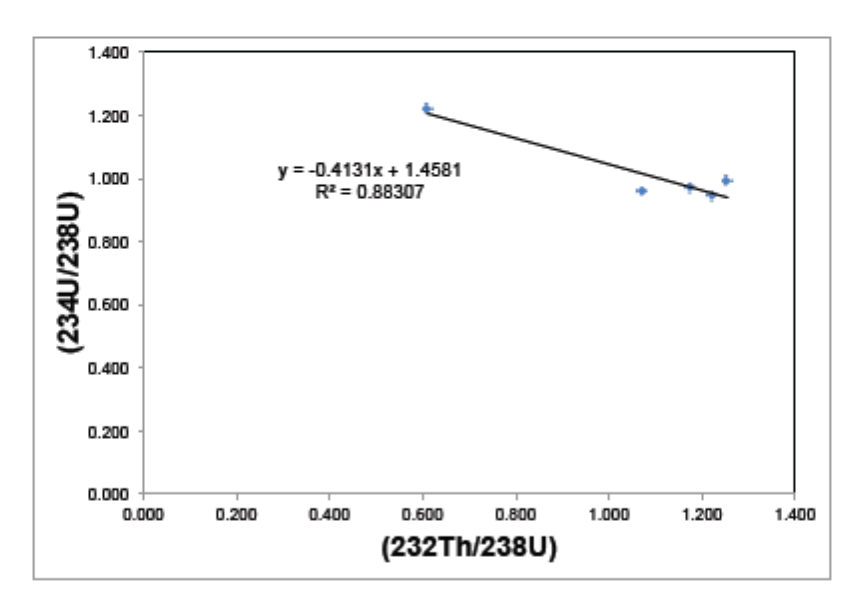
JPT1 40cm Caliche



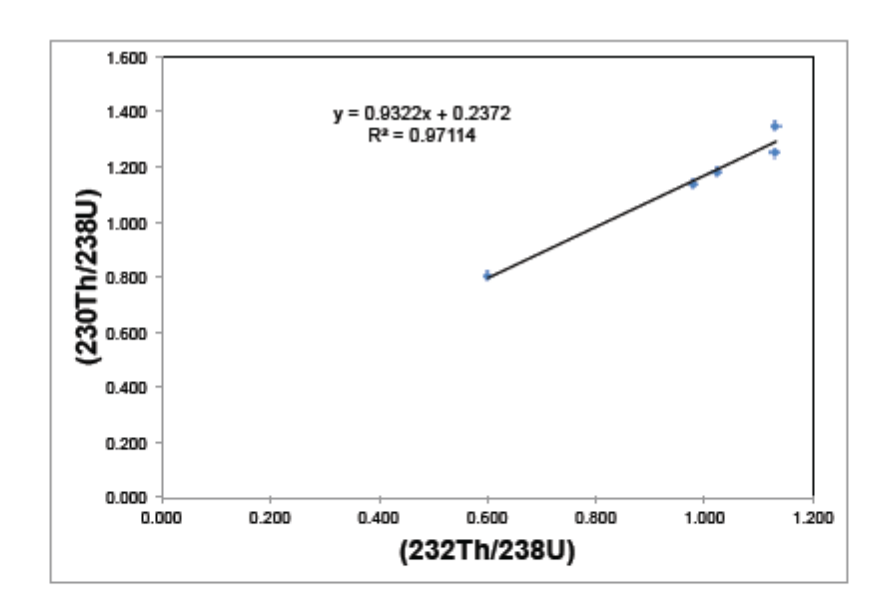


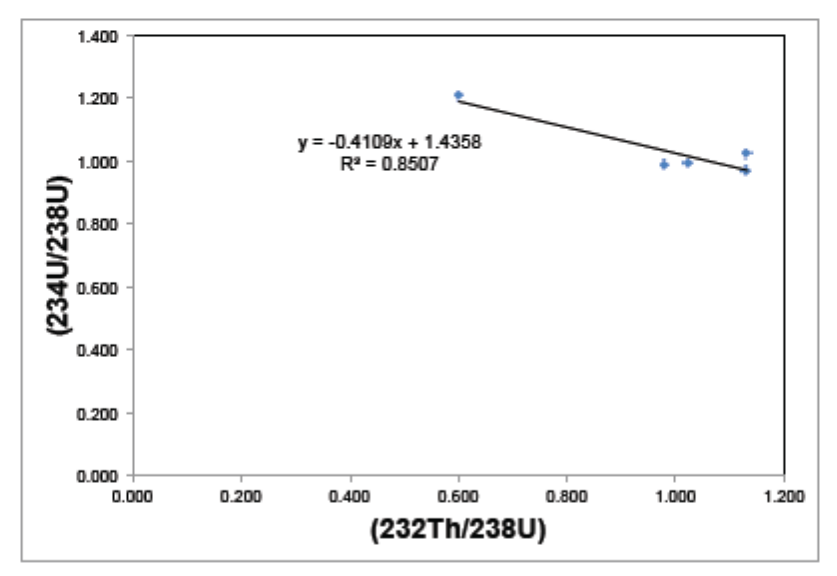
JPT2 0 to 7 cm



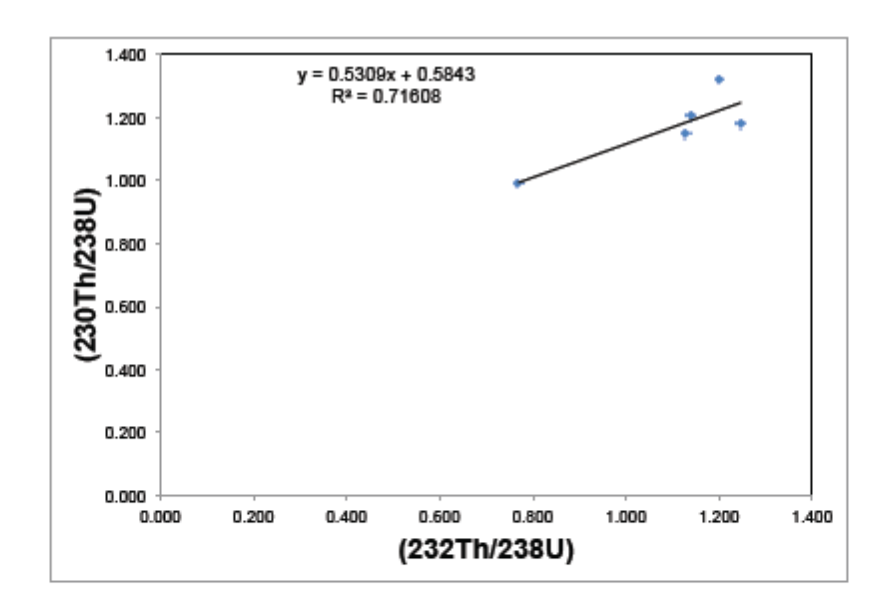


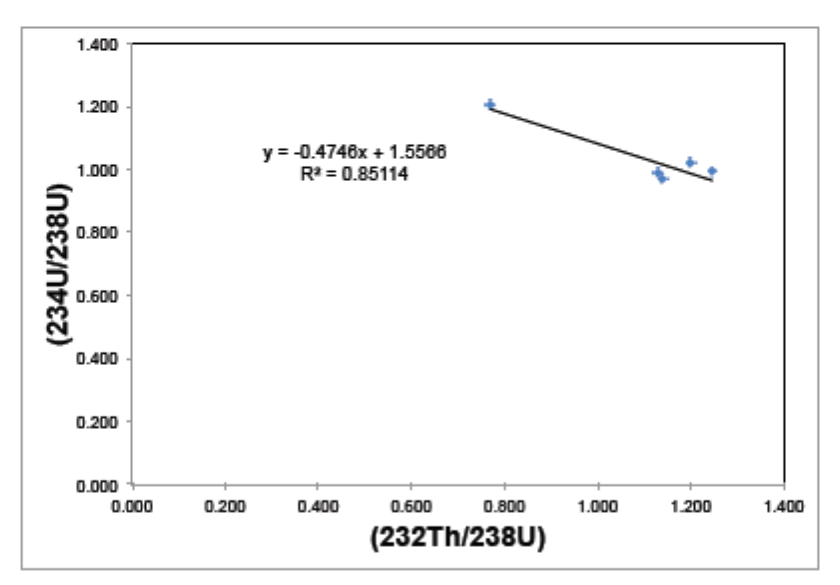
JPT2 7 to 10 cm



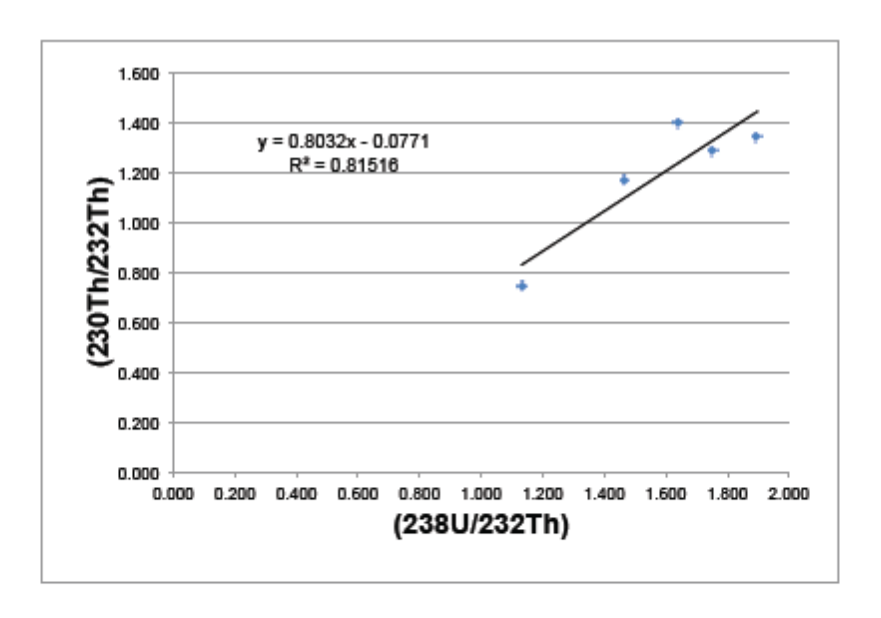


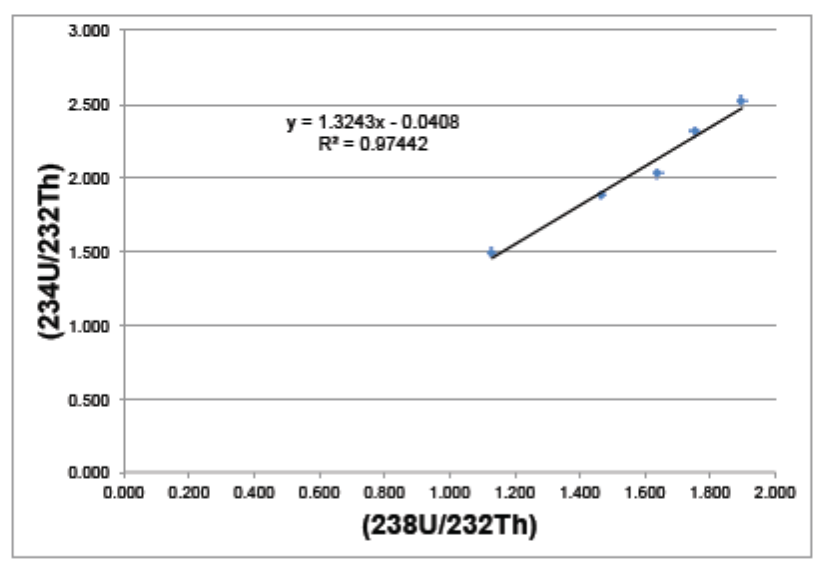
JPT2 27 to 30 cm



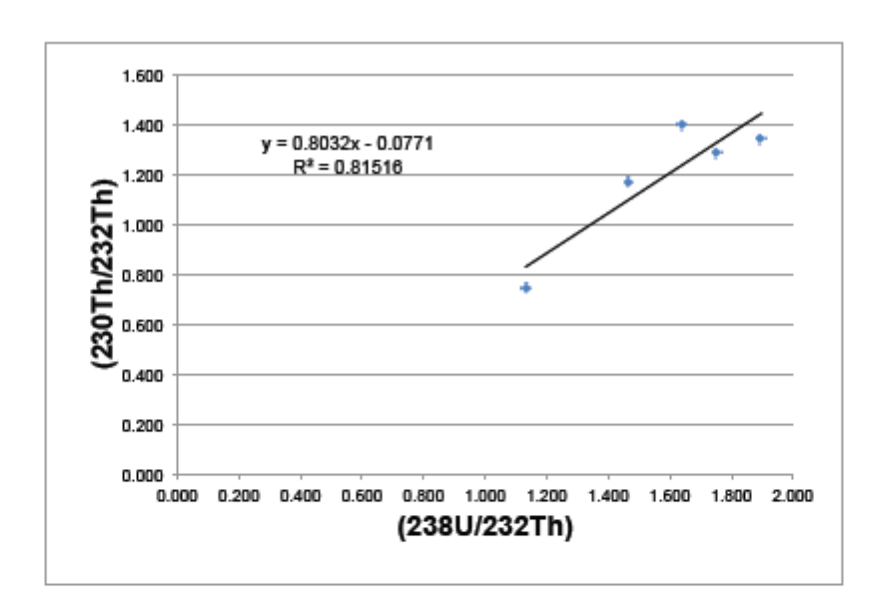


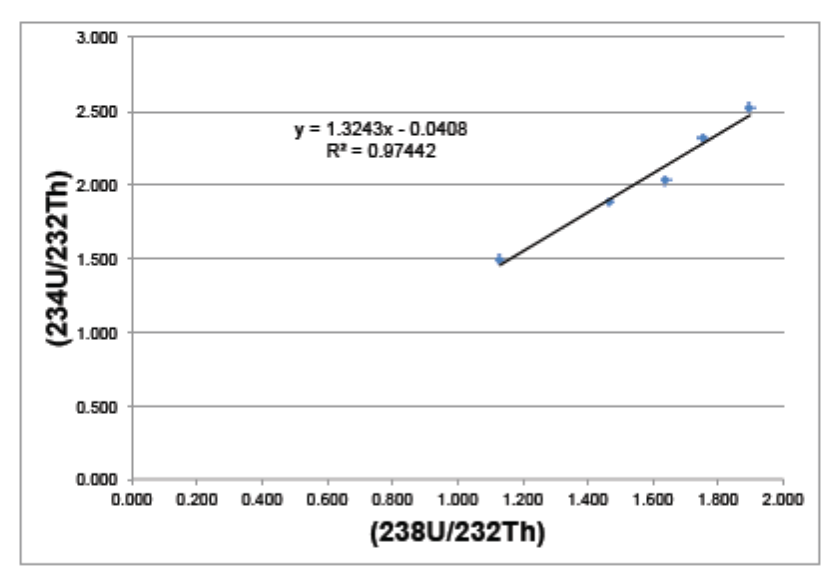
JPT2 37 to 40cm





JPT 2 Caliche 48 cm





JPT 2 Caliche 48 cm